UNCLASSIFIED

AD 290 308

Reproduced
by the

ARMED SERVICES TECHNICAL INFORMATION AGENCY
ARLINGTON HALL STATION
ARLINGTON 12, VIRGINIA

UNCLASSIFIED

NOTICE: When government or other drawings, specifications or other data are used for any purpose other than in connection with a definitely related government procurement operation, the U. S. Government thereby incurs no responsibility, nor any obligation whatsoever; and the fact that the Government may have formulated, furnished, or in any way supplied the said drawings, specifications, or other data is not to be regarded by implication or otherwise as in any manner licensing the holder or any other person or corporation, or conveying any rights or permission to manufacture, use or sell any patented invention that may in any way be related thereto.

290308
290308
AD No.
ASTIA FILE COPY

I.E.R. 63-1-5
SERIES 72
ISSUE 7

SAND MOVEMENT BY WIND

by

PIERRE-YVES BELLY

ASTIA
RELEASED
DEC 5 1962
TISIA

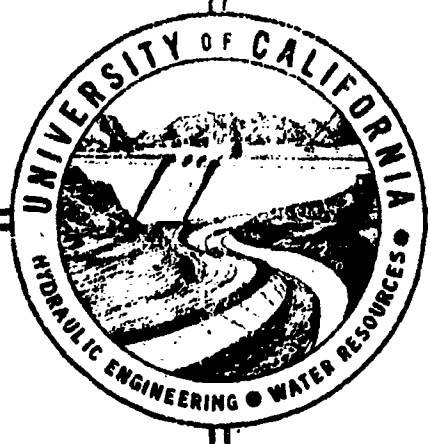

HYDRAULIC ENGINEERING LABORATORY
WAVE RESEARCH PROJECTS

UNIVERSITY OF CALIFORNIA
BERKELEY

University of California
Hydraulic Engineering Laboratory
Wave Research Projects

Submitted under Contract DA-49-055-eng 17 with the Beach Erosion Board, Corps of Engineers, U. S. Army

Institute of Engineering Research
Technical Report
Series 72 Issue 7

SAND MOVEMENT BY WIND

by

Pierre-Yves Belly

Berkeley, California
July, 1962

TABLE OF CONTENTS

Series 72
Issue 7

INTRODUCTION

Sand movement by wind action has already been treated by several research workers. In the following sections, some facts and theories related to the subject of sand movement by wind will be briefly presented.

1. Wind velocity above a sand surface.

The shear stress, τ, produced at the sand surface by wind is one of the most important factors in investigating sand movement by wind action. When the shear stress exceeds a critical value, the sand particles start to move. When sand is being transported, the air above the sand surface behaves as a heavy and non-homogeneous fluid, so that the wind velocity distribution is changed, although the basic equation remains the same.

As long as there is no sand movement, the wind velocity distribution can be adequately described by the general equation,

$$U = C \log \frac{Z}{Z_0}$$

in which U is the velocity at height Z above the sand surface and Z_0 is a reference parameter. The coefficient C, according to Von Karman's

development [6], is equal to $\frac{2.3}{K} U_*$, where K is the Karman Constant, U_* is the shear velocity defined as $\sqrt{\frac{\tau}{\rho}}$, and ρ is the density of air. Taking the value of 0.40 for K, the Von Karman equation can be formulated as,

$$U = 5.75\ U_* \log \frac{Z}{Z_o} .$$

Concerning the roughness factor, Z_o, Zingg [4] proposes the equation,

$$Z_o = 0.081 \log \frac{d}{0.18}$$

with Z_o and the sand grain diameter, d, expressed in millimeters. This equation contains both the results of Bagnold [2] ($Z_o = \frac{d}{30}$) for small grain sizes, and that of White [8] ($Z_o = \frac{d}{9}$) for large grain sizes.

Once the wind velocity is great enough to move sand particles, the wind velocity distribution is altered by the sand movement. Plotted on semi-log paper, the velocity distributions remain straight lines, but, as shown by Bagnold, they all seem to meet at a certain point, which he called "a focus". The height of the focus, Z', appears to be associated with the height of the ripples which form on the surface, in a way somewhat analogous to that in which Z_o is associated with the dimensions of the grains. For a sand of average grain size 0.25 mm; Bagnold found the height of the focus, Z', to be about 3 mm, and the corresponding velocity to be about 2.5 m/sec. A more thorough study made by Zingg [4] allows one to predict the focus by means of the formulae,

$$Z' = 10\ d \text{ millimeters}$$

$$U' = 20\ d \text{ miles/hour}$$

where the grain diameter, d, is expressed in millimeters. Using the components of the focus, Z' and U', the wind velocity distribution can be expressed by,

$$U = C \log \frac{Z}{Z'} + U' .$$

Bagnold assumed a coefficient C of 5.75 U_*, which corresponds to the value of 0.40 for the Karman Constant. But experiments by Zingg [4] yielded the equation,

$$U = 6.13\ U_* \log \frac{Z}{Z} + U'$$

which indicates a value of 0.375 for the Karman Constant.

2. Sand movement by wind.

When the wind above a sand surface is great enough, the particles start moving. The wind velocity profile and the shear velocity are the primary motivating factors in iniating and sustaining sand movement. The initiation of sand movement has been theoretically investigated by Bagnold [2]. He obtained for the threshold value of the shear velocity,

$$U_{*t} = A\sqrt{\frac{\sigma\ \rho}{\rho}\ g\ d},$$

where d is the grain diameter, g is the acceleration of gravity, σ and ρ are specific weights of sand and air, respectively. Bagnold found that the coefficient A is nearly constant for a sand diameter of 0.25 mm and for all sands of larger grain size. A approximates 0.1. Experiments by Zingg [4] corroborate this result. For very small grains (when the Reynolds number $U_* d/\nu$ is less than the critical value 3.5, i.e. when

the surface becomes "smooth") the value of the coefficient A is no longer constant. Fig. 1 shows the variation of the threshold velocity with grain size as found by Bagnold.

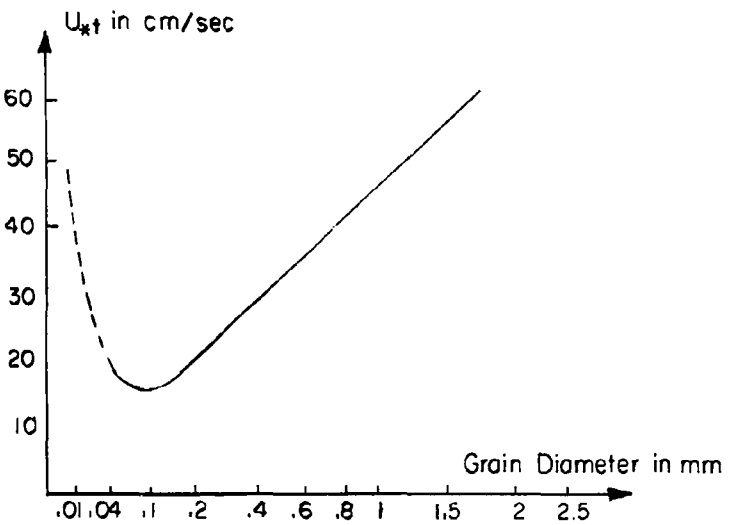

FIGURE I- INITIATION OF SAND MOVEMENT

The theories on sand movement can be classified into two groups. One is based on the investigation of the vertical distribution of the sand movement above the bed, and the other is based on the assumption that the sand particles move downstream with bouncing motions near the sand surface. Representative of the former concept are theories of Kawamura and of Ishihara and Iwagaki (see reference 1); experimental results correspond well with the above theories, and the total rate of transport could be obtained by integration with respect to the height, but the expressions

are too complicated for practical use. The Bagnold and Kawamura formulae are obtained by using the latter theories, and are expressed below.

Bagnold formula[2]

The rate of sand movement per unit width and unit time, q, is given by,

$$q = C\sqrt{\frac{d}{D}}\ \frac{\rho}{g}\ U_*^3$$

where D is the grain diameter of a standard 0.25 mm sand, d is the grain diameter of the sand in question, ρ is the specific weight of the air ($\frac{\rho}{g} = 1.25\ 10^{-6}$ c.g.s.), U_* is the shear velocity and C has the following values:

1.5 for a nearly uniform sand

1.8 for a naturally graded sand

2.8 for a sand with a very wide range of grain sizes.

Kawamura formula[3]

The rate of sand movement, q, is given by,

$$q = k\ \frac{\rho}{g}\ (U_* - U_{*t})\ \ (U_* + U_{*t})^2$$

where ρ is the specific weight of air, U_* is the shear velocity, U_{*t} is the threshold shear velocity, and k is a constant which should be determined by experiment. For a sand of average grain size 0.25 mm, Kawamura obtained k = 2.78 in a wind tunnel.

The basic ideas of the above formulae are almost the same, and

except for light winds, both relationships give approximately the same results if a suitable constant is chosen. On the contrary, as shown by Fig. 2, experimental results obtained in wind tunnels by Bagnold and Kawamura differ widely, although the sand diameter was almost the same. Experimental results obtained in wind tunnels by Zingg[4] and Horikawa[1] are also plotted on Fig. 2. From his results Zingg modified the Bagnold formula thus,

$$q = C\left(\frac{d}{D}\right)^{3/4} \frac{\rho}{g} U_*^3$$

with C = 0.83

In addition to these theoretical formulae, O'Brien[8] and Rindlaub proposed the following formula from data derived in the field:

$$G = 0.036\ U_5^{\ 3} \quad (\text{for } U_5 \ \ 20 \text{ ft/sec})$$

where G is the rate of transport in pounds per day per foot width, and U_5 is the wind velocity 5 ft. above the sand surface in ft/sec.

Confirmation of these formulae by field results is not particularly good, but since there is considerable scatter in the experimental data, these formulae are still useful in the description of a particular condition when a suitable constant is chosen.

3. Flying distance of sand particles.

Mathematical approaches to this problem have been made by Bagnold[2] and Ford[7]. Photographic observation of the sand path con-

firmed theoretical results in both cases. From the sand distribution in a horizontal trap, Kawamura[3] and Horikawa[1] derived the average flying distance of the sand particles. Experimental values are plotted in Fig. 3.

4. Sand traps.

Experiments by Horikawa and Shen[1] demonstrated that none of the available sand traps used by previous investigators gave entirely satisfactory results. They showed that the efficiency of a horizontal trap can be made relatively high, simply by making the trap reasonably long. As for the vertical type of sand trap, they developed one in which the disturbance of the flow is minimum; the efficiency approaches 100%, and it can be used for experiments in wind tunnels as well as for field experiments. This vertical trap is described later.

EXPERIMENTAL APPARATUS AND PROCEDURE

Experiments were conducted in a wind tunnel located in Building 276 at the Richmond Field Station of the University of California. This tunnel, 4 ft. wide, 2.5 ft. high, and 100 ft. long, was constructed of plywood; the lower part of one side was made of glass for observation (Fig. 4 and 5). The wind was generated by a fan at the exit end. The mean velocity was varied from 24 to 40 ft/sec by a rheostat controlling the fan speed.

Wind velocities were measured with a standard Prandtl type pitot tube which was attached to a point gage and introduced into the air stream through the top of the flume. The pitot tube was connected to a Magnehelic gage having a range of one half inch of water and graduated into divisions of 0.02 inches. The Magnehelic gage was chosen instead of an Ellison draft gage, because its response to pressure changes is more rapid.

The mean diameter of the sand used in this experiment was 0.44 mm, as shown by the mechanical analysis curve in Fig. 6a and 6b. The sand was spread over a length of 62 ft. of the flume, with a thickness of 2 inches. A hopper was placed at the entrance of the flume, for use during long runs, and the feed-in adjusted to the rate of transport.

The vertical trap developed by Horikawa and Shen[1] was placed in the center of the flume 7 ft. before the end of the sand bed. This trap

had a width of 3/8 inch and a height of 1 ft. (Fig. 9). A horizontal trap 8 ft. long, consisting of 18 compartments was permanently fixed at the end of the sand bed. In order to avoid the side wall effect the amount of sand retained in the trap was measured only in the center part of the flume over a width of 2 ft.

The desired wind velocity was obtained by adjusting the rheostat of the speed control on the fan. Each run was allowed to continue for a period of 5 to 30 minutes. The ripples on the bed and the scour around the vertical trap were observed. At the end of each run the horizontal trap was cleaned out with a vacuum cleaner (Fig. 5).

EXPERIMENTAL RESULTS AND DISCUSSION

Velocity distribution on sand surface

In order to investigate the side wall effect on wind velocity, the wind velocity distributions in a cross section were measured. The transverse profiles, 11 ft. before the end of the sand bed are shown in Fig. 10 for different fan currents. These transverse profiles show the wind to be practically uniform across the channel except in the close proximity of the walls.

Vertical wind profiles were measured at the same place (11 ft. before the end of the sand bed) at the center of the flume. The velocity distributions obtained for different fan currents are shown in Fig. 11, and plotted on semi-log scale in Fig. 12 and 13.

For wind velocities less than the critical value required to initiate sand movement, the relationship between wind velocity and height above the sand surface obeys the logarithmic law (Fig. 12).

For wind velocities larger than the critical value, the relationship also obeys the logarithmic law above the focal point (Fig. 13). The focal point located at,

$$Z' = 0.015 \text{ ft.}$$

$$U' = 13 \text{ ft/sec}$$

seems to agree with Zingg's estimate of,

$$Z' = 10\,d \text{ mm}$$

$$U' = 20\,d \text{ miles per hour}$$

where d is the mean diameter of the sand in millimeters, or:

$$Z' = 0.0135 \text{ ft.}$$

$$U' = 13 \text{ ft/sec}$$

The shear velocity U_* can be determined by the slope of the velocity distributions in Fig. 13. The values of U_* for different wind velocities (measured at Z = 1.0 ft. above the sand bed), calculated from Zingg's formula,

$$U = 6.13\, U_* \log \frac{Z}{Z'} + U' ,$$

are given in Table 1.

Table 1

Wind velocity (at Z = 1.0 ft.) in ft/sec	Shear velocity U_* in cm/sec
25.0	39.0
25.7	37.5
26.0	42.2
27.0	43.8
28.2	46.3
30.0	47.6
31.0	51.0
32.8	55.5
34.5	58.5
39.0	70.0

The relationship between U and U_* is approximately linear (Fig. 14). The shear velocity, U_*, for other wind velocities was determined by using this graph.

The value of the threshold velocity is radically changed by the

presence or the absence of a sand feed-in. Without sand feed-in U_{*t} = 40 cm/sec, but with sand feed-in the threshold velocity is greatly lowered: U_{*t} = 30 cm/sec. The latter value is very close to the value calculated with the Bagnold's formula (U_{*t} = 34 cm/sec).

Rate of sand transport

The amount of sand caught by the horizontal trap was measured for velocities varying from the threshold value to 37 ft/sec. The sand feeding which was located at the upstream end of the sand bed is a very important factor in sand movement for lower wind velocities. The sand feeding greatly lowers the threshold velocity and at the same time changes the amount of sand transported for lower velocities. Table 2a gives the data obtained without sand feeding. Table 2b gives the results obtained when the sand feeding was established with a discharge approximating the rate of sand transport. These results are plotted in Fig. 15 and in Fig. 16 to show the comparison with those of Bagnold, Kawamura and Horikawa.

The apparent reversal of the curve obtained without sand feeding is perhaps due to the fact that the sand used in this study has a wide range of grain sizes (0.2 to 0.7 mm). At, or near the threshold it is possible that the action of the smaller grains was impeded by the larger, thus modifying the over-all values for the threshold and rate of transport. More preciesly, near the threshold the sand grains move mainly by saltation. Since the surface layer remains practically immobile (no surface creep), the smaller grains are hidden by the larger ones and as a result the sand behaves as it had a much larger mean diameter. According

to the Bagnold formulae for the rate of transport and the threshold value of the shear velocity, the curves for two different mean diameters are as sketched below:

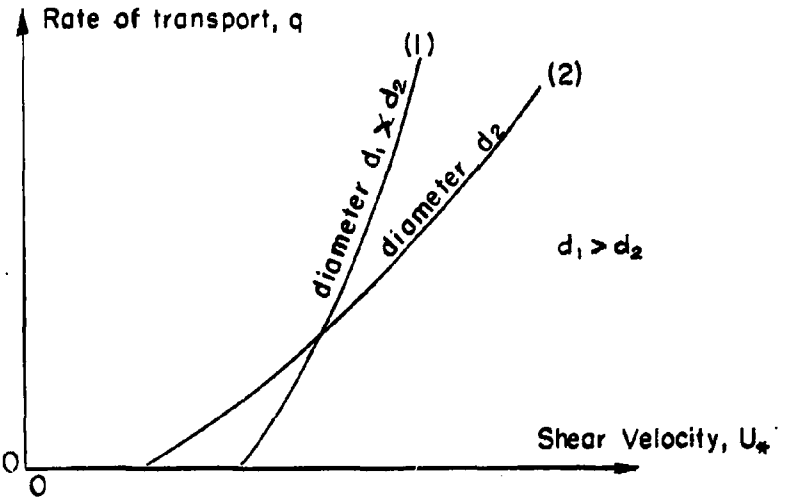

Therefore the sand which initially follows curve (1), gradually changes its effective mean diameter and begins to follow curve (2). This phenomena which is related to the state of the surface layer, disappears when this surface layer is artificially set in motion by the sand feed-in. Therefore no anomaly is noted in the resulting curve.

The experimental values for the maximum rate of transport (i.e. with sand feed-in), q, can be compared to the values predicted from the Bagnold and Kawamura formulae.

For the average grain size, d = 0.44 mm, the Bagnold formula gives in c.g.s. units,

$$q = C \sqrt{\frac{0.44}{0.25}} \times 1.25 \times 10^{-6} \times U_*^{\,3}$$

Taking C = 2.5 (Bagnold proposes 1.8 for normally graded sand and 2.8 for a sand of a very wide range of grain size), this formula is plotted in Fig. 17. Except for wind velocities approaching the threshold, which in any case cannot be described by Bagnold's formula, the agreement with experimental results is very good.

The Kawamura formula is in c.g.s. units,

$$q = k \times 1.25 \times 10^{-6} \times (U_* - U_{*t})(U_* + U_{*t})^2$$

With sand feed-in we found U_{*t} to be about 30 cm/sec. Putting this value in the Kawamura formula and using k = 3.1, this formula describes very well the rate of sand transport for the whole range of velocities (Fig. 18).

Thus, by giving to the constants adequate values, the formulae of Bagnold and Kawamura agree very well with the results obtained.

Table 2a

Wind velocity (at Z = 1.0 ft.) in ft/sec	Shear velocity in cm/sec	Rate of transport in gr/cm-sec
25.0	39	none
26.0	41	0.143
26.0	41	0.012
26.2	42	0.066
26.8	43	0.137
27.0	43	0.096
27.0	43	0.303
27.2	44	0.187
27.8	45	0.313
27.9	45	0.292
28.3	46	0.386
28.5	46	0.382
30.5	50	0.505
30.8	51	0.545
31.0	52	0.580
32.7	54	0.700
33.0	55	0.780
34.8	58	0.910
37.0	64	1.18

Table 2b

Wind velocity (at Z = 1.0 ft.) in ft/sec	Shear velocity in cm/sec	Rate of transport in gr/cm-sec
20.0	30	0.012
23.0	35	0.105
24.8	38	0.182
25.0	39	0.220
26.0	41	0.232
28.4	46	0.380
34.0	50	0.506

Efficiency of the vertical sand trap

The efficiency of the vertical sand trap was tested for various velocities in the course of experiments on the rate of transport. The

horizontal trap was long enough to catch practically all of the sand transported by the wind and served as a reference for the vertical trap. The efficiency of the vertical sand trap is defined as,

$$\eta\ \% = \frac{\text{amount of sand caught in vertical trap}}{\text{amount of sand caught in horizontal trap}} \times 100$$

Table 3 and Fig. 19 give the efficiency η for different wind velocities.

Table 3

Wind velocity in ft/sec	Vert. trap q in gr/cm-sec	Hor. trap q in gr/cm-sec	Efficiency %
25.8	0.084	0.143	60
26.0	0.004	0.116	38
27.0	0.26	0.30	87
27.0	0.022	0.096	23
27.8	0.267	0.313	85
28.3	0.340	0.386	88
28.5	0.314	0.382	83
30:5	0.48	0.505	95
31.0	0.53	0.58	92
31.5	0.51	0.51	100
31.5	0.48	0.50	105
32.0	0.65	0.69	107
32.0	0.58	0.61	106
35.0	0.90	0.98	110
35.0	1.01	1.13	112
35.0	0.94	1.02	108
35.5	0.98	1.15	118

An efficiency higher than 100% probably is due to the small amount of unmeasured sand which fell beyond the horizontal trap, and also to the possibility of secondary currents in the proximity of the mouth of the vertical trap. In any case the vertical trap has a sufficiently good efficiency for velocities between 30 and 35 ft/sec to avoid the necessity of

corrections in later experiments.

Almost immediately after the beginning of a run, a scour takes place around and below the vertical trap as shown on Fig. 8. This scour seems to remain steady and therefore does not influence the measurements. For runs of long duration, however, the platform becomes undermined, and this is probably a cause of error, for the surface creep does not thereafter enter the mouth of the trap, as sketched below:

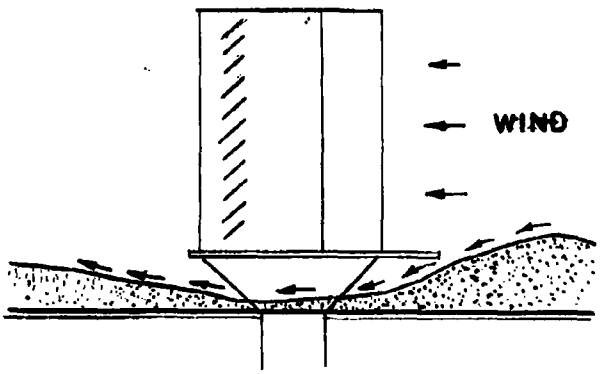

This phenomenon which occurs for a run duration of about one hour was avoided as much as possible by using run times of 5 to 15 minutes (except in the last part of the experiment where runs had durations of 30 to 45 minutes).

For higher velocities, the grain size distribution of the sand caught in the vertical trap is very close to the grain size distribution of the bed (Fig. 20). The relative absence of bigger grains in the sand caught by the vertical trap is probably caused by the platform of the trap which can sometimes be an obstacle to surface creep. For velocities approaching the threshold value, the grain size distribution in the vertical

trap shows a distinct lack of the larger grains (Fig. 21). This fact cannot be entirely attributed to the inefficiency of the vertical trap and probably indicates the manner in which the sand is moving near threshold (the large grains not taking part in the general movement).

Ripples on sand surface

The ripples produced on the sand surface were observed during the different parts of the experiment. They appear on a flat sand surface as soon as there is some sand movement and they disappear at very high velocities (about 36 ft/sec). The wave lengths of the ripples were measured for different wind velocities but as shown in Fig. 22, there is no clear correspondence between wave length and wind velocity. The average wave length is:

$$\lambda = 3 \text{ inches}.$$

Average flying distance

First, consider a sand surface of unit width, over which the wind is blowing, as shown in Fig. 24

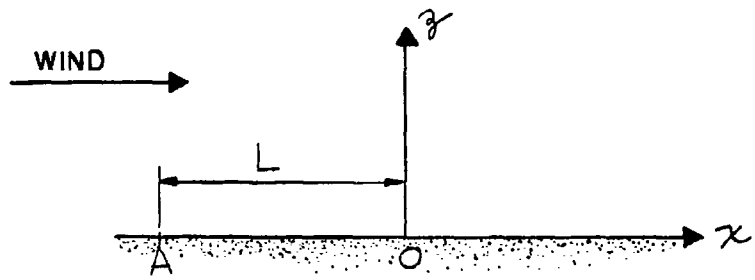

Fig. 24

The x-axis is taken in the direction of the wind. If G_o is the amount of sand falling on a unit area of sand surface during unit time, the amount of sand "jumping" from the surface of unit width and of length dx is: $G_o.dx$. If we assume now that all the particles have the same flying distance, L, the sand particles which pass over the section (O) are jumping from the sand surface between the sections (O) and (A), with OA = L. Therefore the amount of sand passing through the cross section (O) per unit time is,

$$q = \int_o^L G_o.dx = G_o.L$$

Thus the average flying distance is,

$$L = \frac{q}{G_o}$$

q, the rate of transport has been already obtained by the experiment

G_o, which may be considered as the amount of sand falling per unit width and unit time, in a trap of infinitely small length placed immediately after the end of the sand bed, can be obtained by extrapolating the curve of sand distribution in the horizontal trap for x = O.

As the first trap has a length of 0.5 foot, the percentage of sand from the surface creep is very small, and therefore it is unnecessary to correct the curve of sand distribution, so that the amount of sand transported by saltation can be blended with the total rate of transport, q.

From Figures 25, 26 and 27 we have:

For U = 28 ft/sec, G_o = 58 lb/ft^2-hour, and $L = \frac{q}{G_o}$ = 1.30 ft.

For U = 31 ft/sec, G_o = 90 lb/ft^2-hour, and $L = \frac{q}{G_o}$ = 1.35 ft.

For U = 35 ft/sec, G_o = 140 lb/ft^2-hour, and $L = \frac{q}{G_o}$ = 1.5 ft.

Figures 28 and 29 give G_o and the average flying distance, L, as a function of wind velocity.

For the same values of the velocity but for a sand of 0.25 mm, Bagnold found respectively 2.8, 3 and 5 inches, for the average flying distance. The average flying distance increases with the grain diameter of the sand, but more study should be done to determine if values as large as found in these experiments are reasonable. Also, Bagnold found a remarkable agreement between the average flying distance and the wave length of the ripples produced on the sand surface. As the wave length in the present tests was a constant value of 3 inches, the Bagnold relationship was not verified.

Frequency distribution function of flying length

First, consider the condition as shown in Fig. 30

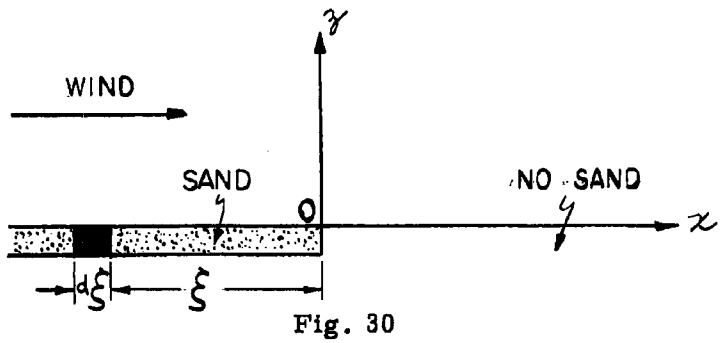

Fig. 30

The x-axis is taken in the direction of the wind and the region of $x < O$ is covered with sand, from where the sand particles are flying and dropping into the sand trap set at $x > O$. The amount of sand falling in the unit area in $x > O$ per unit time, $F(x)$, is the summation of sand particles jumping from the sand surface in the region $x < O$. Therefore if $g(L)$ is the frequency distribution function of the flying length, $F(x)$ is expressed by the following integration,

$$F(x) = G_O \int_{-\infty}^{O} g(x - \xi).d\xi$$

where, as seen before, G_O is the amount of sand falling on the unit area of sand surface during unit time.

If $t = x - \xi$, $F(x)$ can be rewritten such as,

$$F(x) = - G_O \int_{\infty}^{x} g(t)\ dt$$

or,

$$F(x) = - G_O \int_{\infty}^{O} g(t)\ dt - G_O \int_{O}^{x} t(t)\ dt$$

By definition,

$$- \int_{\infty}^{O} g(t)\ dt = 1$$

Therefore,

$$F(x) = G_O \left[1 - \int_{O}^{x} g(t)\ dt \right],$$

Then, the distribution function of flying length is obtained by derivating $F(x)$, with respect to x,

$$g(x) = - \frac{1}{G_o} \cdot \frac{dF(x)}{dx}$$

The functions:

$F(x) = G_o e^{-0.390 x}$, for U = 28 ft/sec

$F(x) = G_o e^{-0.375 x}$, for U = 31 ft/sec

and $F(x) = G_o e^{-0.333 x}$, for U = 35 ft/sec

with x in feet, have been found to fit reasonably the horizontal distribution of sand drift given in Figures 25, 26 and 27. By derivation with respect to x, we find,

$g(x) = - 0.390 e^{-0.390 x}$, for U = 28 ft/sec

$g(x) = - 0.375 e^{-0.375 x}$, for U = 31 ft/sec

$g(x) = - 0.333 e^{-0.333 x}$, for U = 35 ft/sec

These distributions are plotted in Fig. 31.

Variation of the flying distance with grain size

This study can be made by knowing the grain size distribution in the different compartments of the horizontal sand trap. This analysis has been done for the wind velocity of 31 ft/sec.

Table 4 gives the weight of sand (expressed in pounds per hour and per foot width) for each compartment of the horizontal trap, and for each range of grain sizes. The results are plotted in Fig. 32.

Extrapolating the curves for x = O, the amount of sand falling on a unit area of sand surface during unit time, G_o, can be determined, and the average flying distance, L, calculated ($L = q/G_o$) for the different

ranges of grain sizes (Table 5).

As a final result, Fig. 33 shows the variation of the flying distance, L, with grain size.

Table 4

U = 31.5 ft/sec

Dist. in ft.	Distribution for different grain size 200-300μ %	q	300-350μ %	q	350-450μ %	q	450-500μ %	q	500-600μ %	q	600-100μ %	q	TOTAL q
0.5	8.5	3	14.5	5.1	19	6.6	30	10.5	17	6	10	3.5	35
1.0		3.8		5.9		4.2		4		1		0	24
1.5	28	4.2	37	5.6	21	3.1	11	1.65	2	0.3	0	0	15
2.0		3.5		3.0		2.3		0.8		0.1			10
2.5	30	2.2	26	2.0	31	1.8	11	0.8	1	0.075	0	0	7.5
3.0		1.8		1.2		1.2		0.5		0.05			5
3.5	36	1.45	28	1.1	23	0.92	10	0.35	1	0.035	0	0	4
4.0		1.3		0.7		0.7		0.1		0			2.5
5.0	62	1.25	25	0.5	11	0.22	15	0.03	0	0	0	0	2
7.0	74	1.5	16	0.3	8	0.16	0.02	0	0	0	0	0	2
8	77	0.7	14	0.14	6	0.06	0.7	0.007	0	0			1
Total q		24.8		24.8		21.7		19.0		7.4		4.0	

Note: The amount of sand "q" are in lb/ft/h

The values of q which could not be found in the experimental results have been determined from the curves (Fig. 22).

Table 5

Flying length :

$$L = \frac{q}{G_o}$$

	Grain size in μ .					
	200/300	300 /-350	350/450	450/500	500/600	600/1000
q (lb/ft/h)	24.8	24.9	21.7	19.0	7.4	4.0
G_o (lb/ft^2/h)	5	9	16	28	32	40 (?)
L (ft)	5	2.8	1.35	0.68	0.23	0.1

(G_o = 2 x extrapolated value (obtained for a 1/2 ft. long trap))

Response time of the sand-bed to a change of wind velocity

In order to investigate the response time of the bed to a change of wind velocity, the wind was first allowed to blow over the sand surface for a relatively long time (sufficiently long to observe a duplication of the results on the amount of sand transported, both in the vertical and horizontal traps). The wind velocity then was suddenly changed to a higher value, and the sand collected in the vertical trap was weighed every two minutes, until a duplication of results was observed. The wind velocity then was again adjusted to the previous value, while the same measurements were made at the vertical sand trap. After a sufficiently long time, the wind velocity was again adjusted to the higher value, and the same process repeated. The two particular values of the velocity were:

U = 31.5 ft/sec

U = 35 ft/sec

Table 6

The first velocity was 31 ft/sec, and the second was 35 ft/sec. The figures represent the weight of sand collected in the vertical trap, every two minutes, in grams.

	Time in minutes									
Run No.	2	4	6	8	10	12	14	16	18	20
1	86.5	94	90.5	100	100.5	94	99			
3	86	94	97	96	97.5	99	102			
5	75	79	77.5	78.5	80.5	84	84	73	80	71
7	77	70.5	67	69	70	69.5				
9	70.5	74	69	73						
11	102	96	97	94	91					
13	82	79	90	80	90					

Table 7

The previous velocity was 35 ft/sec, the new one is 31.5 ft/sec

	Time in minutes									
Run No.	2	4	6	8	10	12	14	16	18	20
2	47	49	51	54	51	51.5	51			
4	46.5	48.5	48	44	50	50.5	51.5			
6	44.5	42.5	41	36	38	35	37	43	36	36
8	50	32	43	44	40	45	41	40	38	41
10	35	35	43	38	40					
12	41	49	46	46						
14	28	29	32	30	31					

(measured at Z = 1.0 ft. above the sand surface). The results from these tests are in Tables 6 and 7. There is a considerable scatter especially for the higher velocity. This dispersion probably is due to some extent to the inaccuracy of the wind velocity readings, these velocities being slightly different in corresponding runs. But as the important fact is the rate of transport with respect to time, we can eliminate the part of the dispersion due to differences in the main wind velocity, by considering the discrepancy between the measurements made within the first few minutes of each run, and the average of the last measurements, when equilibrium is reached. Figure 34 shows the rate of sand transport as a function of time with this correction.

The dispersion is greater at the beginning than at the end of a run, but except for a slight increase during the first 4 minutes in most of the runs, no clear-cut tendency can be observed.

Additional runs were made in order to detect a more subtile development. In those runs, the sand was collected at the vertical trap every 30 seconds:

Table 8

First velocity: 31 ft/sec
Second velocity: 35 ft/sec

Run No.	Time in seconds			
	30	60	90	120
15	26	25	26	25
17	19	19	24	24

Table 9

First velocity: 35 ft/sec
Second velocity: 31 ft/sec

Run No.	Time in seconds			
	30	60	90	120
16	10	12	9	10
18	6	7	6	7

Again it was possible to detect immediately a noticeable change in the rate of transport, but no further development. In conclusion it can be said that the sand-bed adjusts itself almost immediately to a new wind velocity.

SUMMARY AND CONCLUSIONS

1. Althouth the grain size of the sand used was very different from that used by Bagnold and Kawamura, these experiments reaffirmed their findings with respect to rate of sand transport.

2. The average flying distance of the sand particles was found to be much greater than that found by previous investigators, but the difference could possibly be due to the method of calculation.

3. The experiments seem to prove that sand movement has a negligible response time to a change in wind velocity.

ACKNOWLEDGEMENTS

The author wishes to express his sincere appreciation to Professor J. W. Johnson under whose general supervision this study was made, and to Professors H. A. Einstein and A. D. K. Laird for their comments and suggestions.

REFERENCES

(1) Beach Erosion Board, Technical Memorandum No. 119. Sand movement by wind, by K. Horikawa and H. W. Shen, 1960.

(2) Bagnold, R. A., The physics of blown sand and desert dunes, Methuen & Co. Ltd., London, 1954.

(3) Kawamura, R., Study on sand movement by wind, Rept. of the Institute of Science and Technology, Univ. of Tokyo, Vol. 5, No. 3/4, Oct. 1951.

(4) Zingg, A. W., Wind tunnel studies of the movement of sedimentary material, Proc. of Fifth Hydraulics Conf., 1952.

(5) Masch, F. D., Mixing and dispersive action of wind waves, Univ. of Calif., Hydraulic Engineering Laboratory, Waves Research Projects, Berkeley, 1961.
(For the wind tunnel used)

(6) Von Karman, T., Turbulence and skin friction, Journ. Aero. Science, Vol. 1, Jan. 1934.

(7) Ford, E. F., The transport of sand by wind, Trans. A. G. U. Vol. 38, No. 2, April 1957.

(8) O'Brien, M. P., and B. D. Rindlaub, The transportation of sand by wind, Civil Engineering, May 1936.

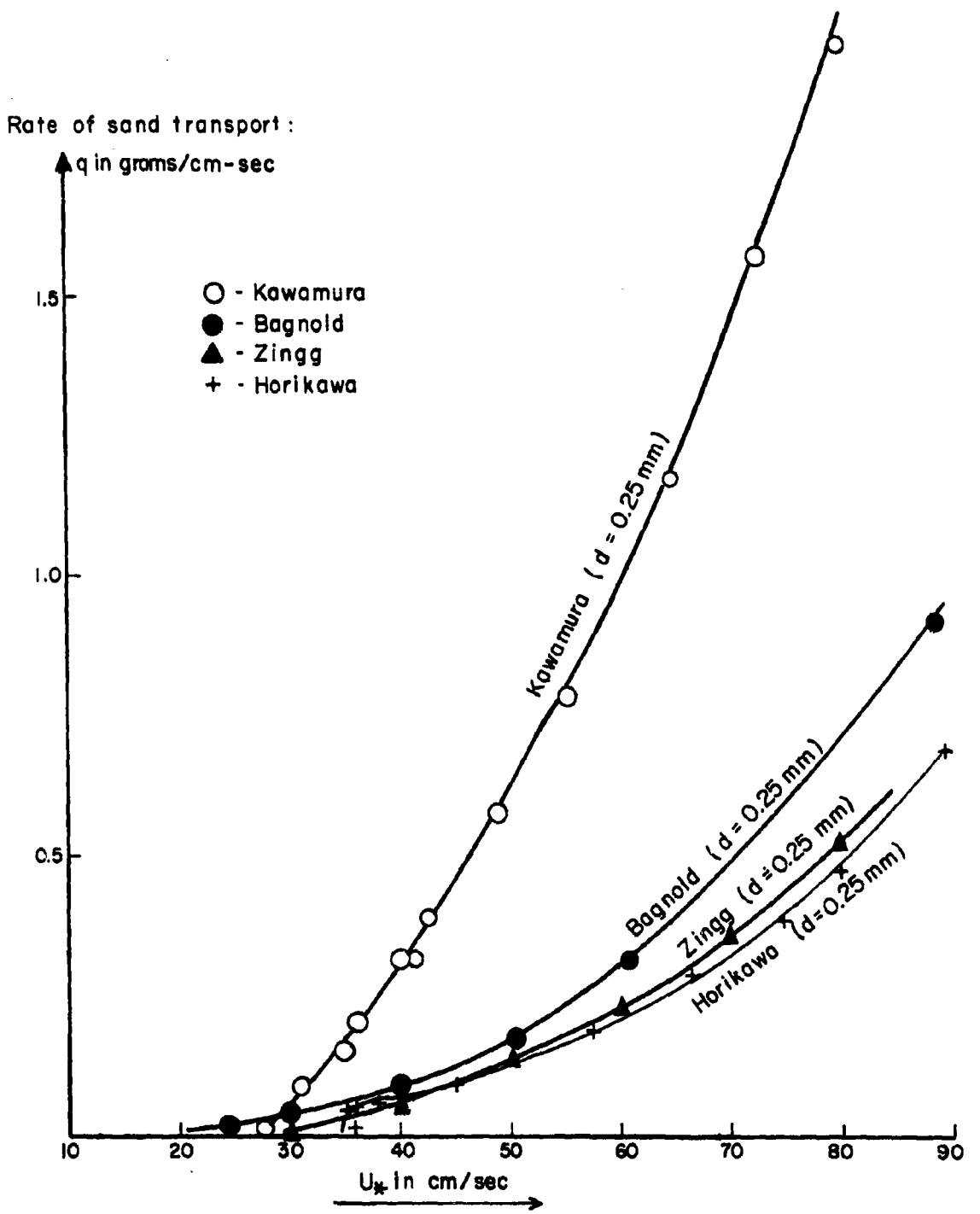

FIGURE 2 - EXPERIMENTAL RESULTS ON SAND TRANSPORT

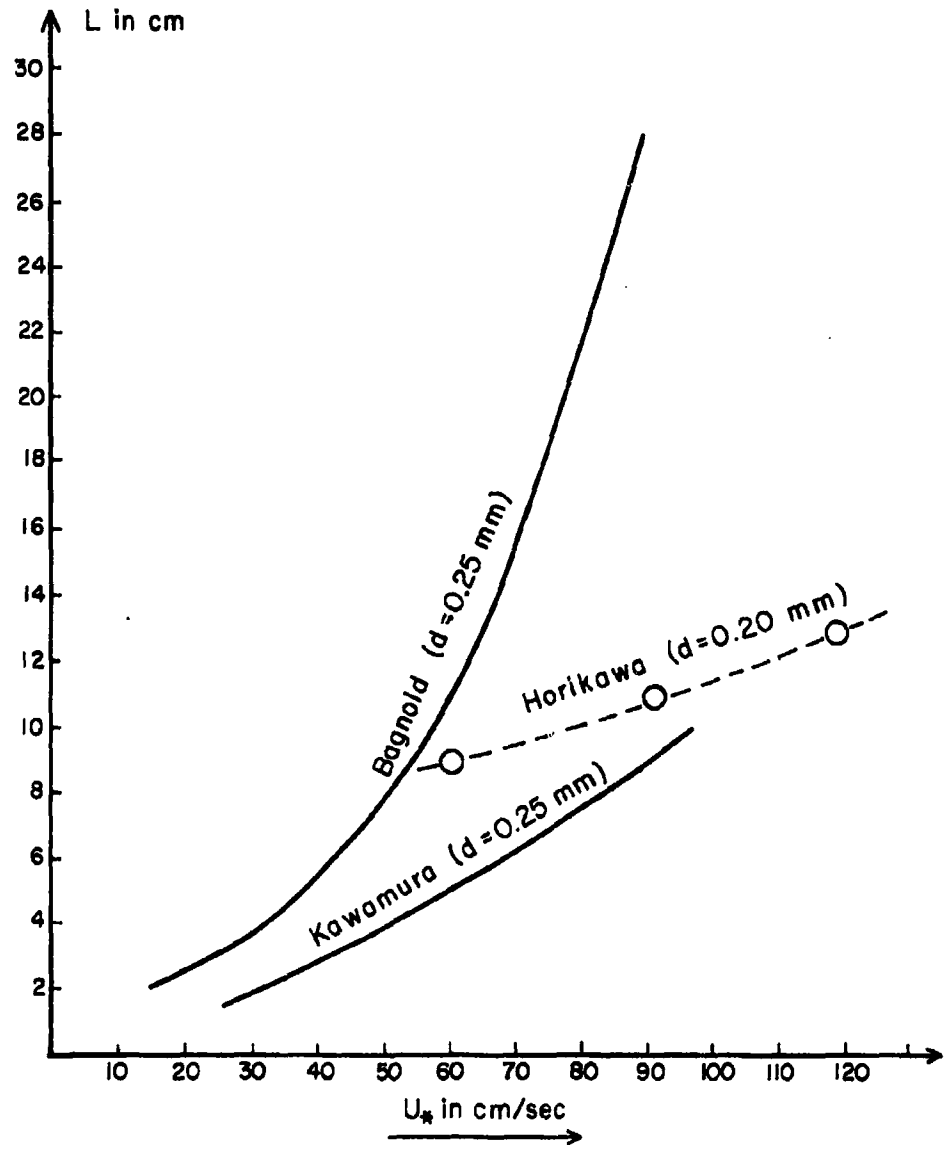

FIGURE 3 - FLYING DISTANCE

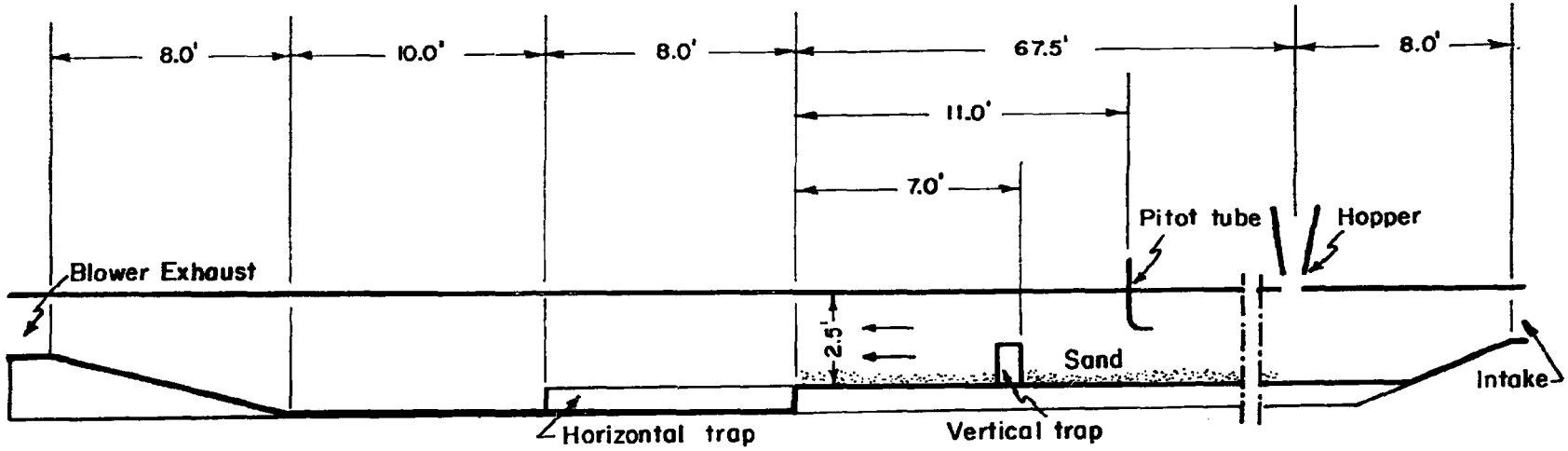

FIGURE 4 - WIND TUNNEL

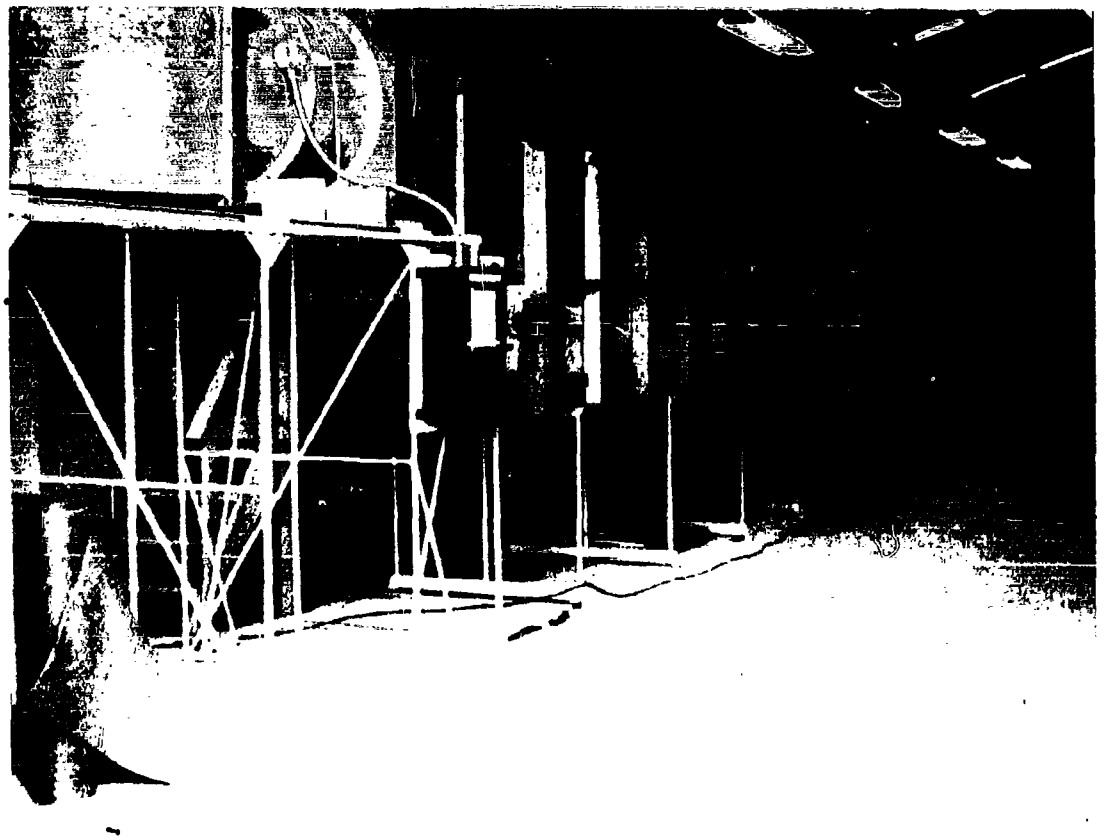

FIGURE 5 - WIND TUNNEL

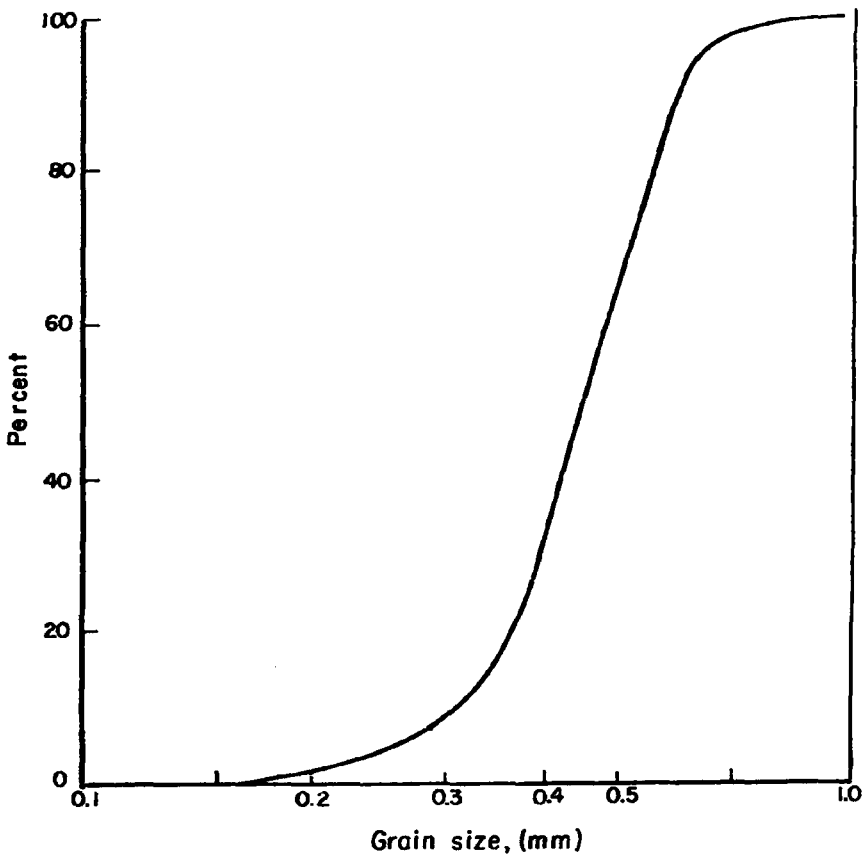

FIGURE 6a - Mechanical Analysis of Sand Used

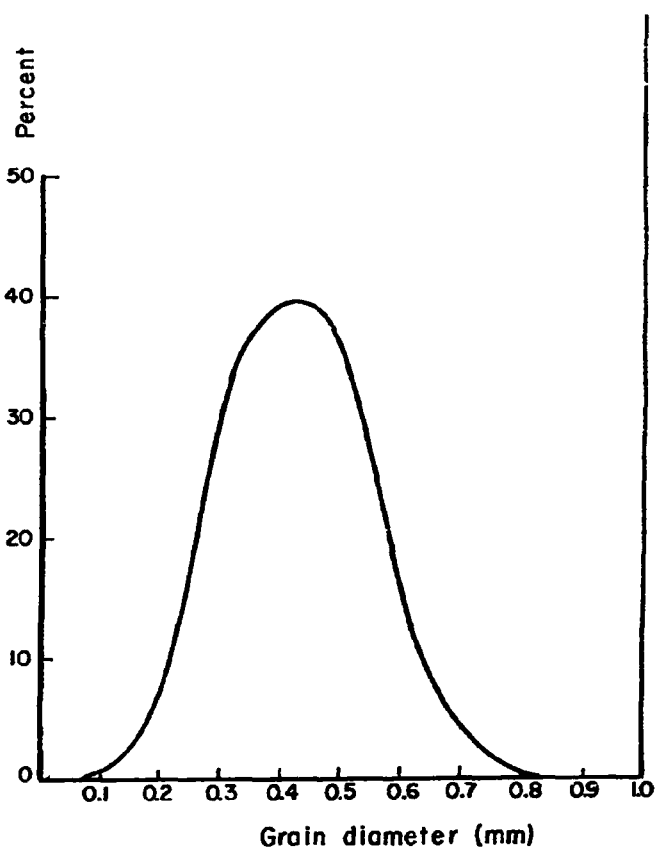

FIGURE 6b - Grain Size Distribution

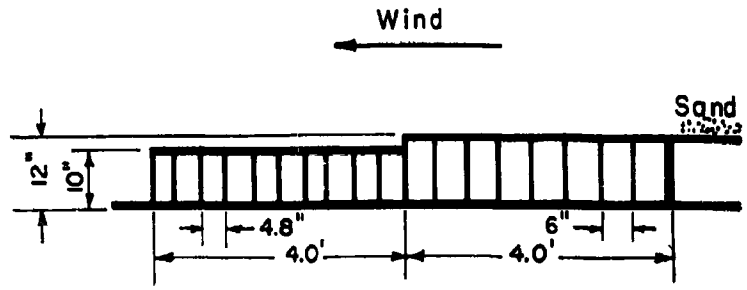

FIGURE 7 - HORIZONTAL SAND TRAP

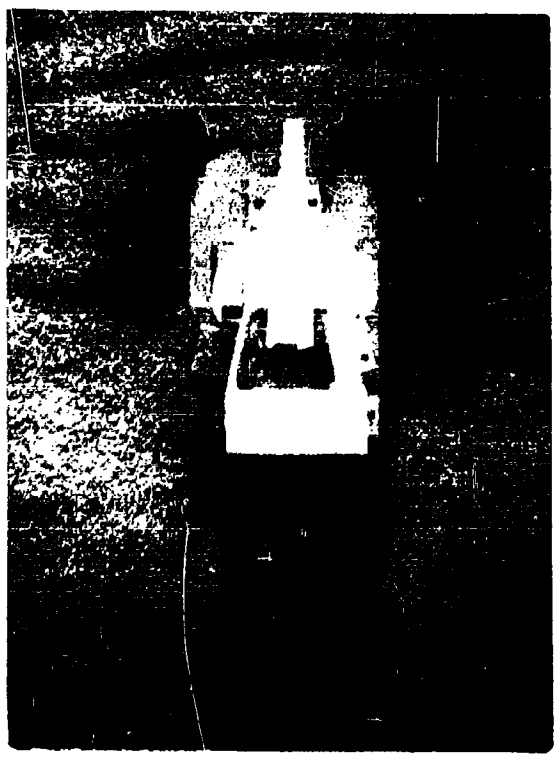

FIGURE 8 - SCOUR AROUND THE VERTICAL SAND TRAP

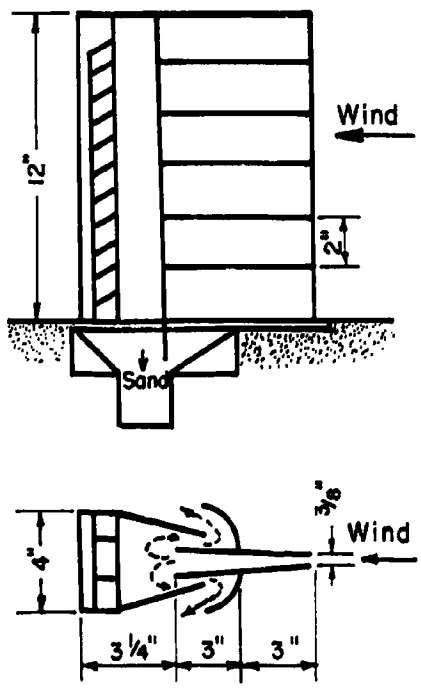

FIGURE 9 -VERTICAL TRAP

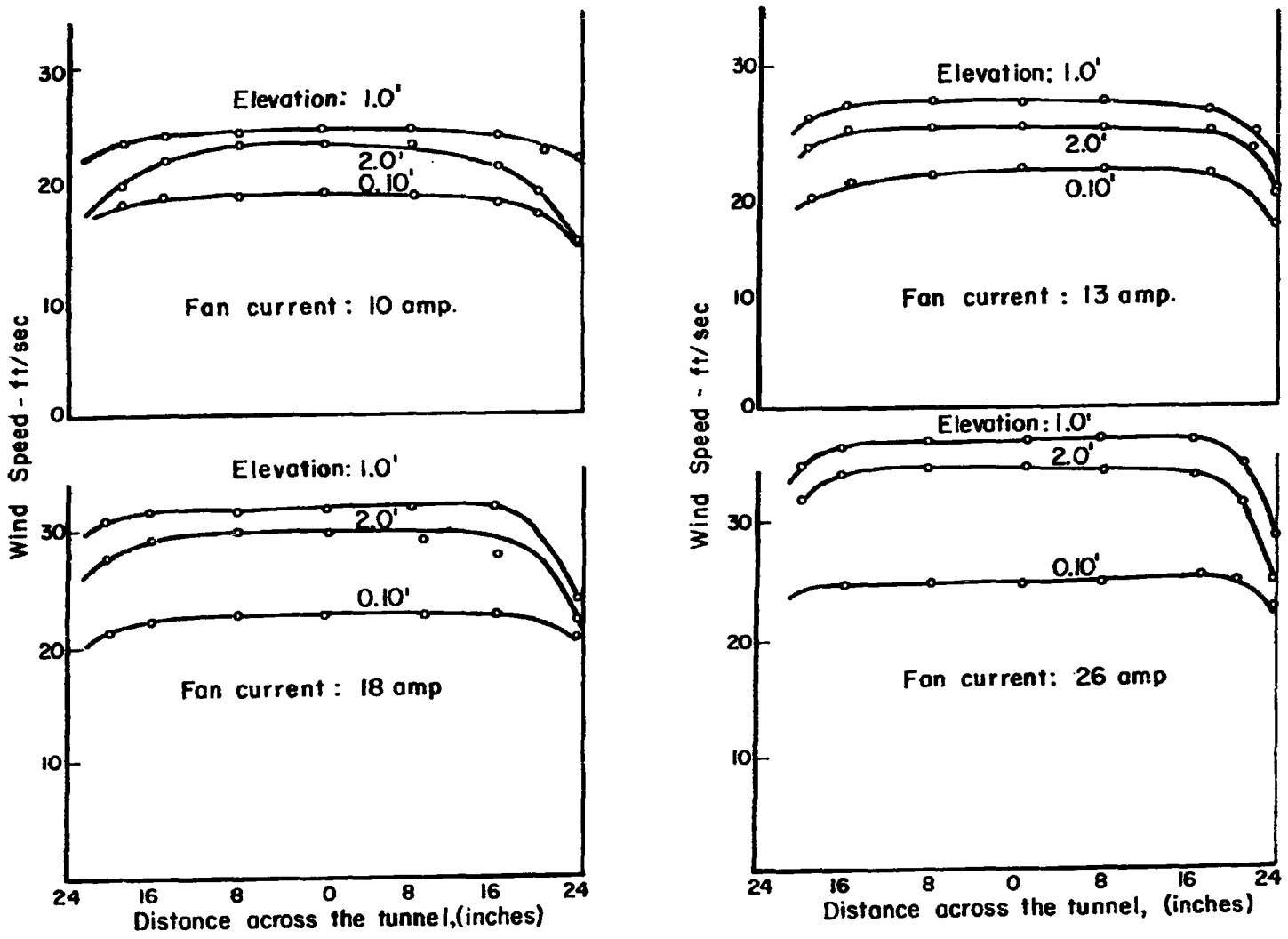

FIGURE 10 - TRANSVERSE PROFILES

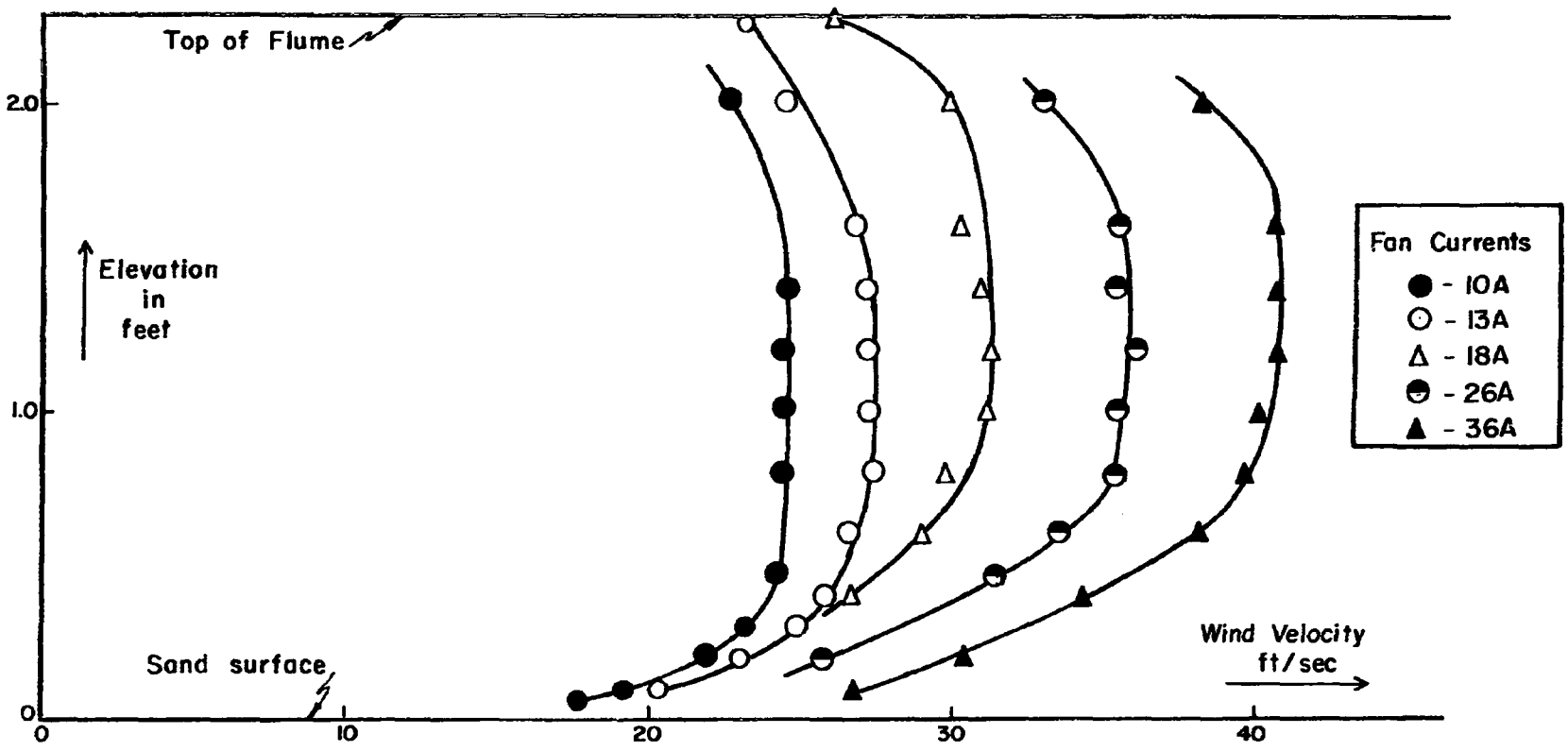

FIGURE 11 - VERTICAL WIND PROFILES

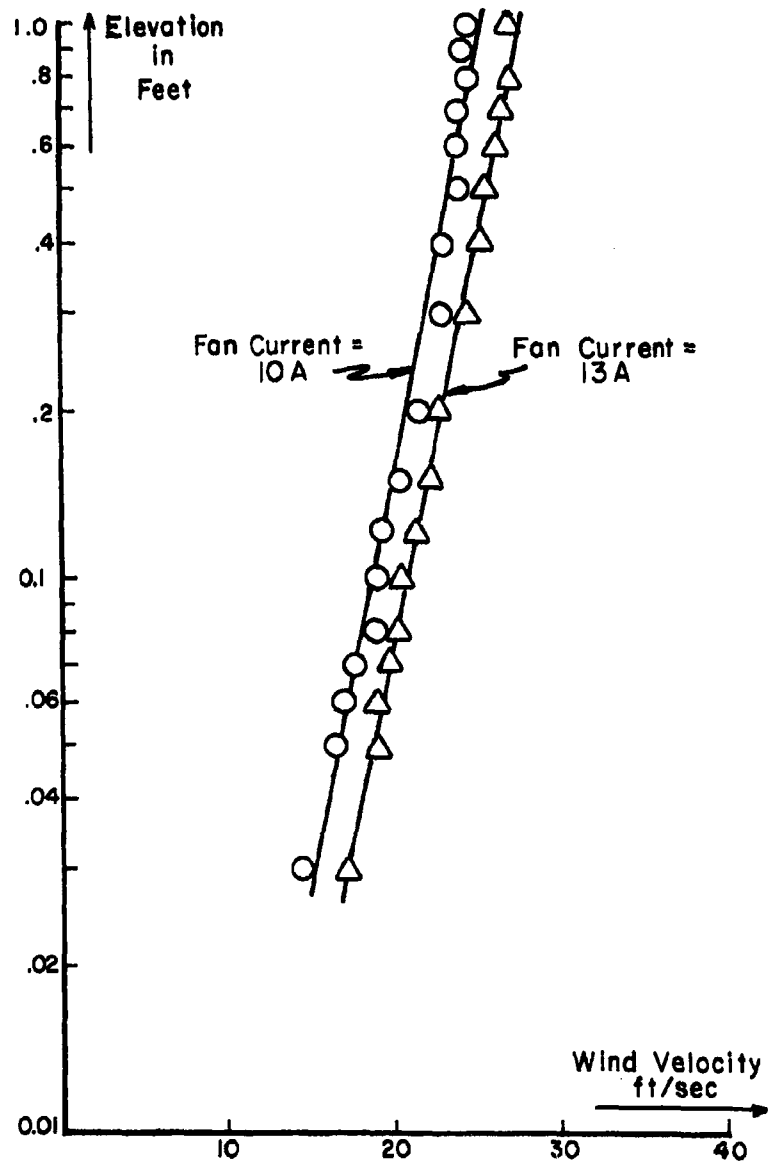

FIGURE 12 - VELOCITY DISTRIBUTION ABOVE SAND SURFACE (NO SAND MOVEMENT)

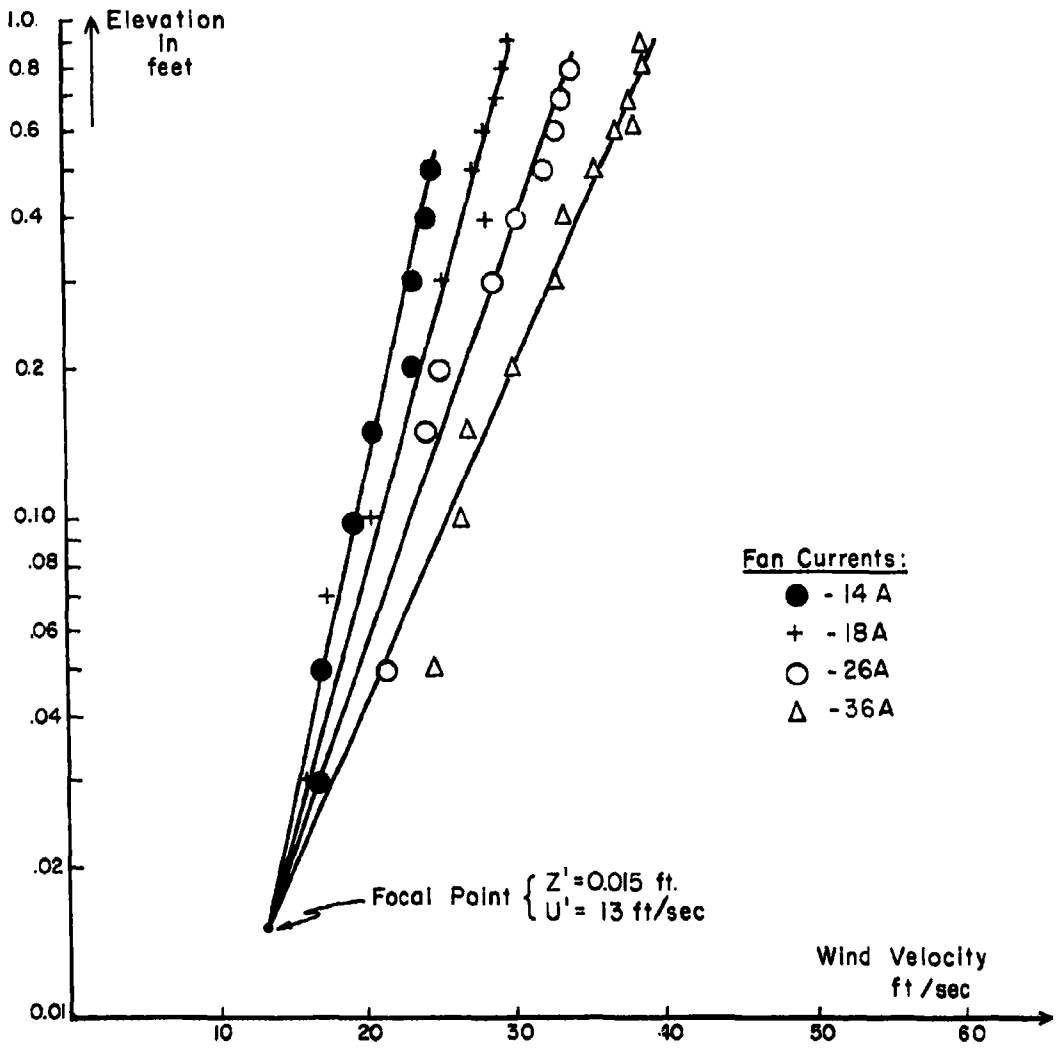

FIGURE 13 - VELOCITY DISTRIBUTION ABOVE SAND SURFACE (WITH SAND MOVEMENT)

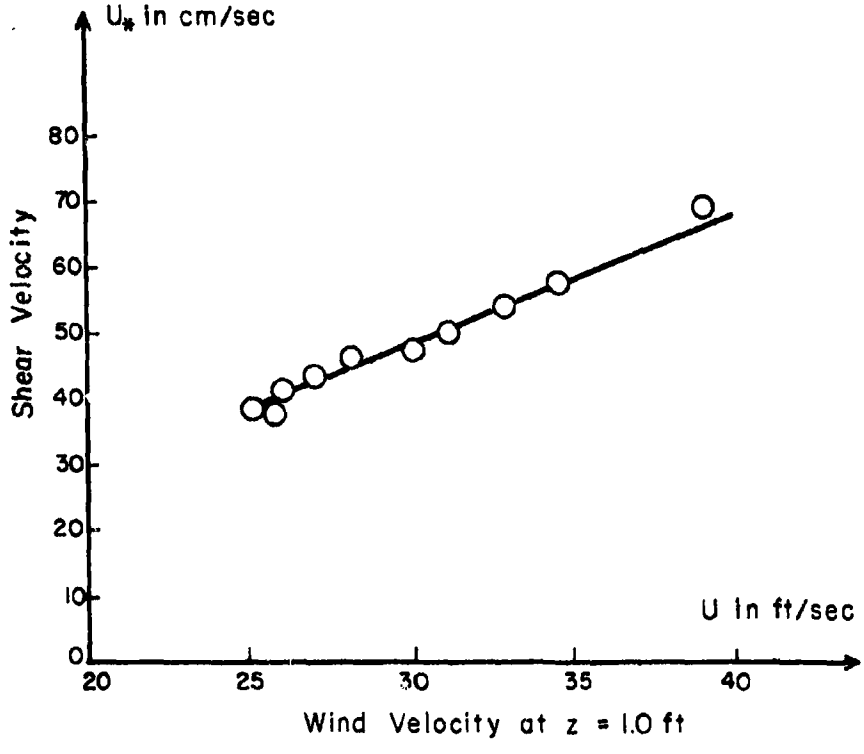

FIGURE 14 - RELATIONSHIP BETWEEN THE MAIN VELOCITY U, AND THE SHEAR VELOCITY U_*.

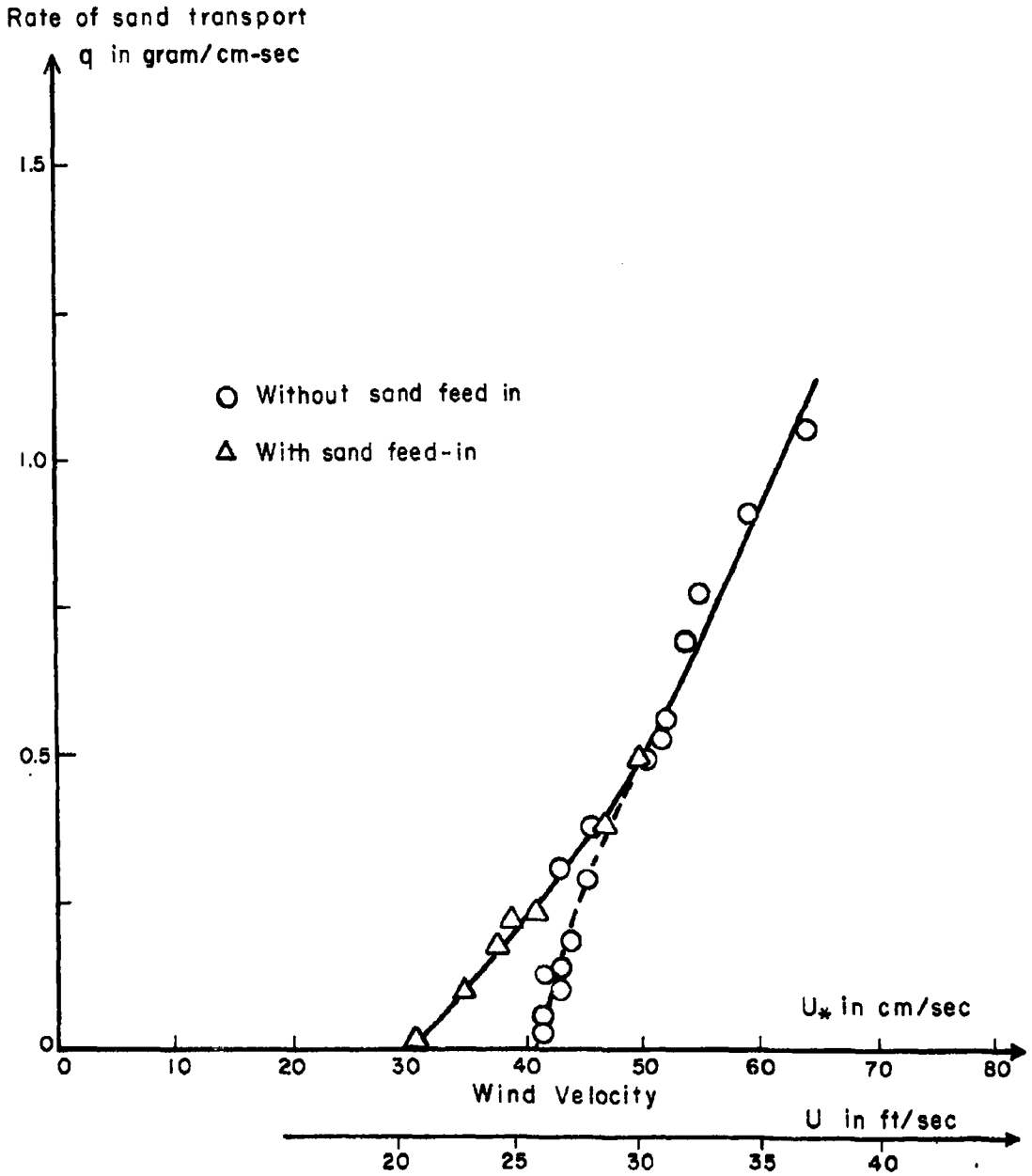

FIGURE 15- EXPERIMENTAL RESULTS ON SAND TRANSPORT

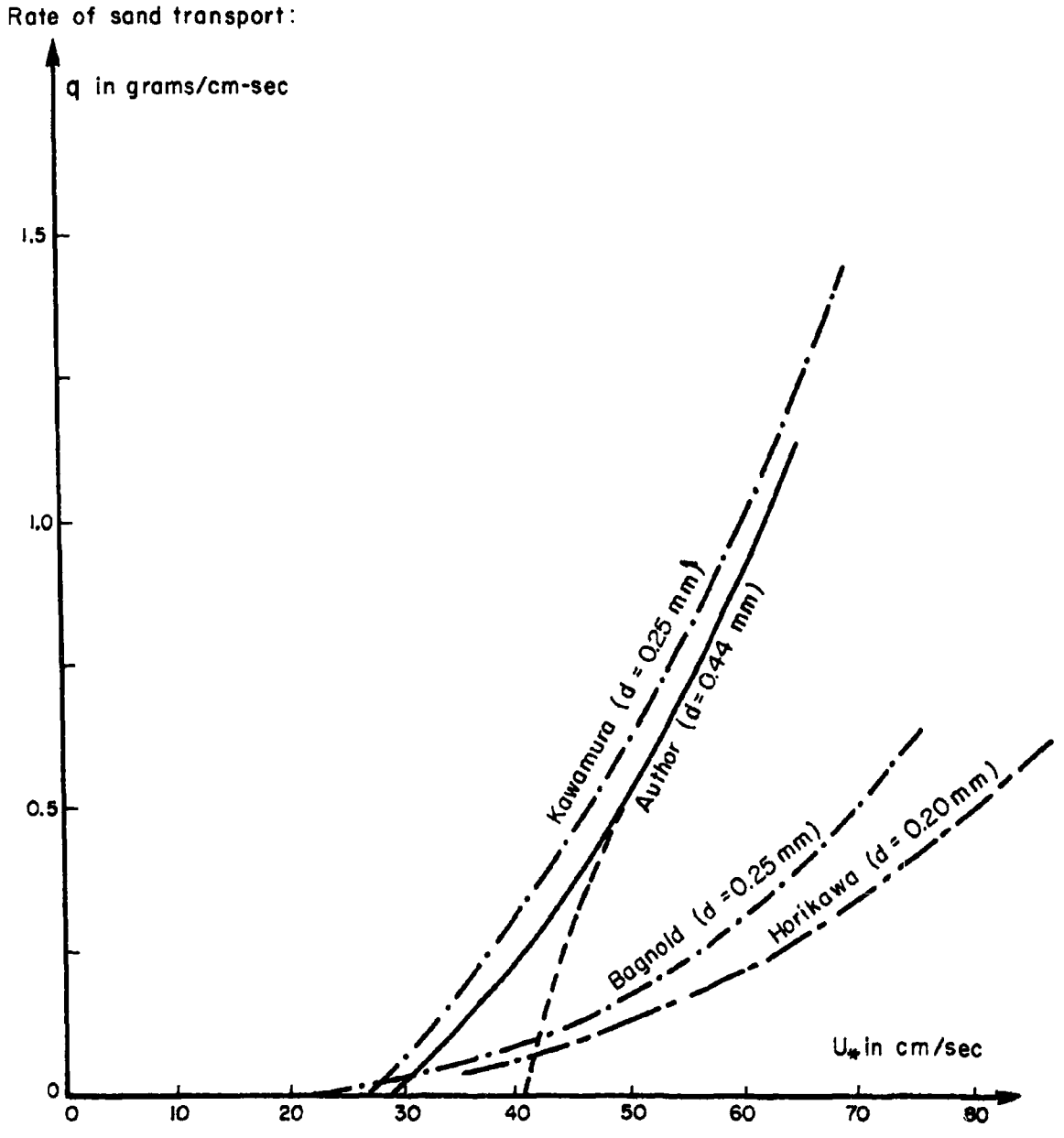

FIGURE 16 - EXPERIMENTAL RESULTS ON SAND TRANSPORT

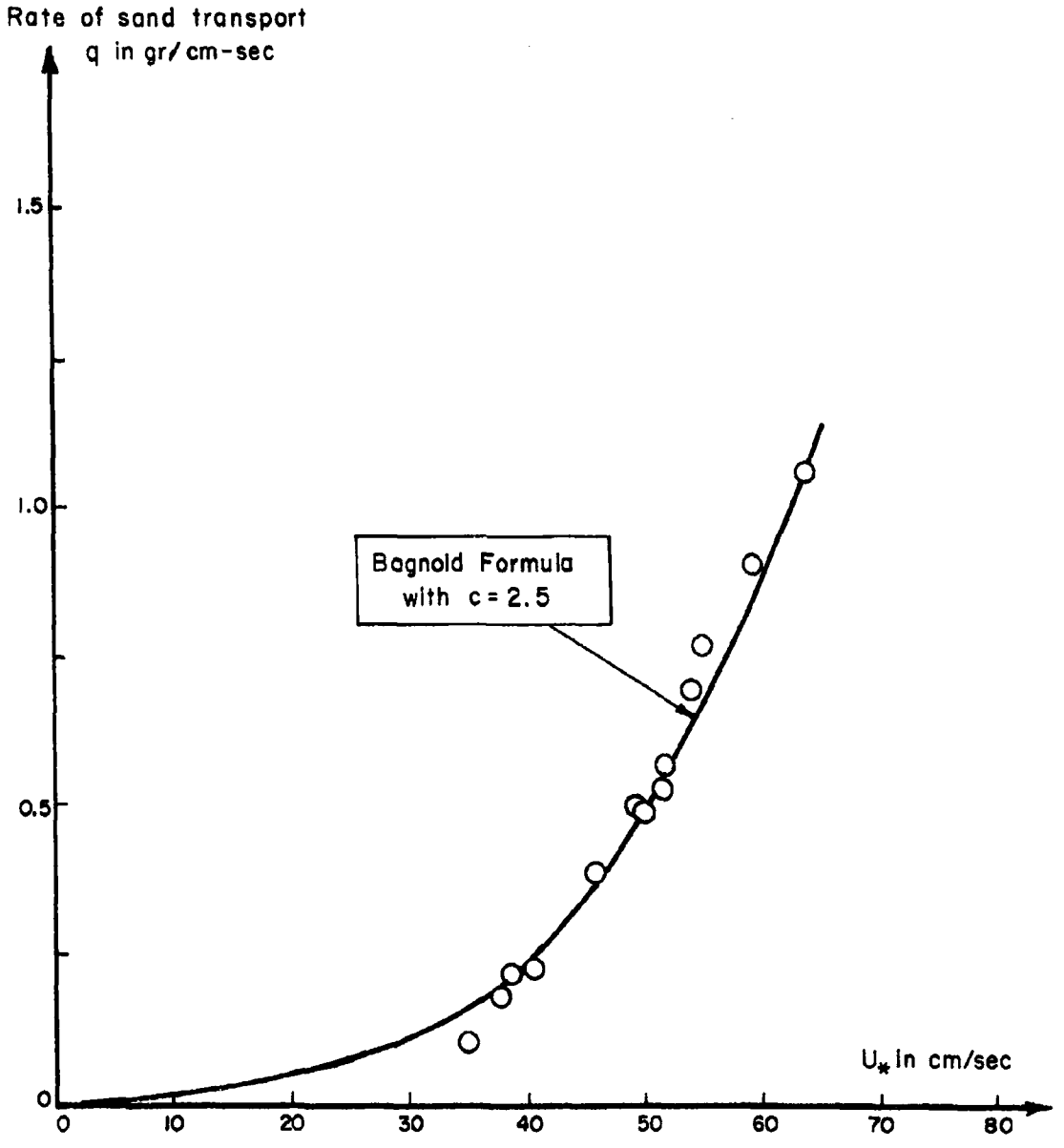

FIGURE 17 - COMPARISON BETWEEN EXPERIMENTAL RESULTS AND BAGNOLD FORMULA

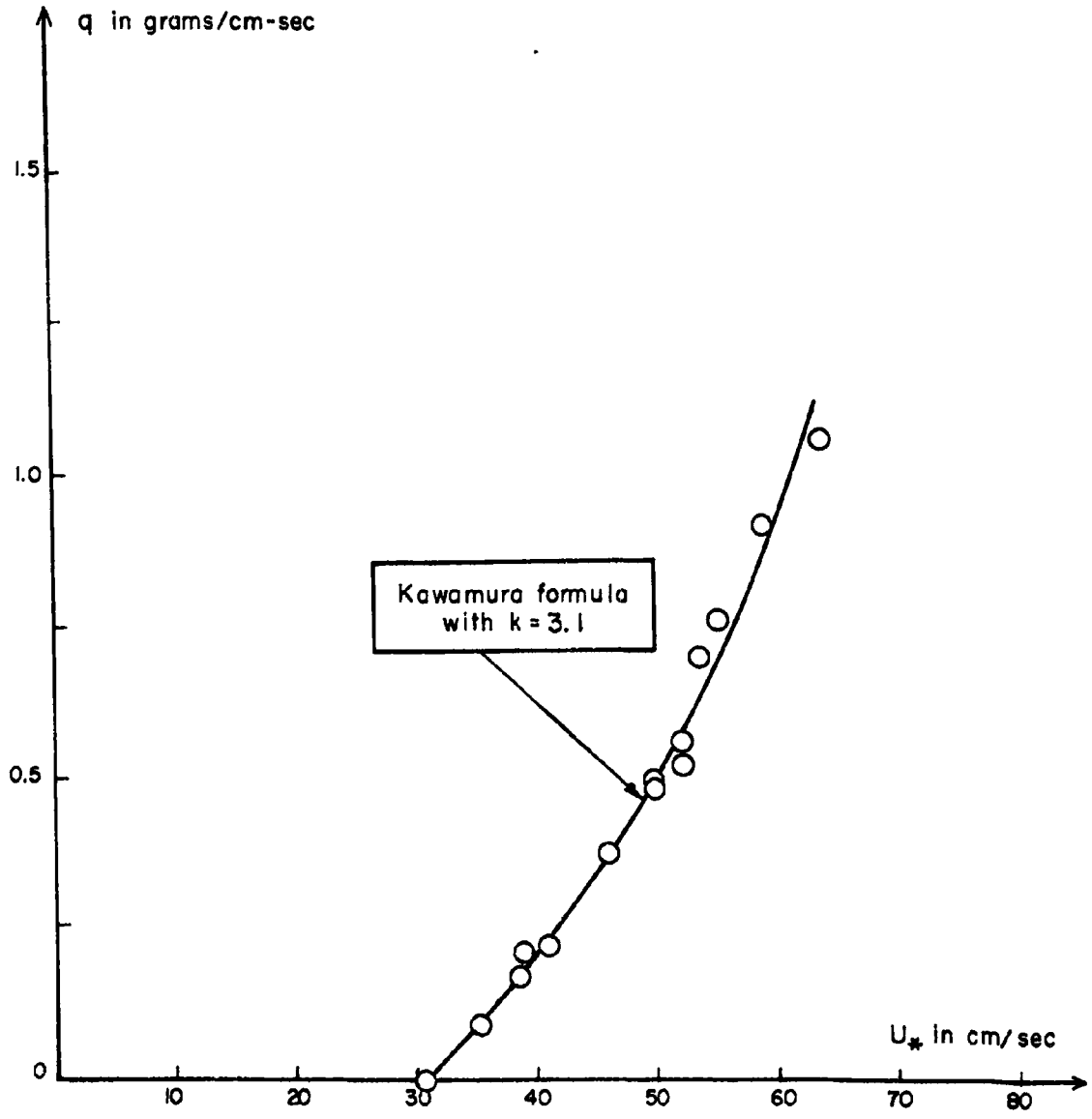

FIGURE 18- COMPARISON BETWEEN EXPERIMENTAL RESULTS AND THE KAWAMURA FORMULA

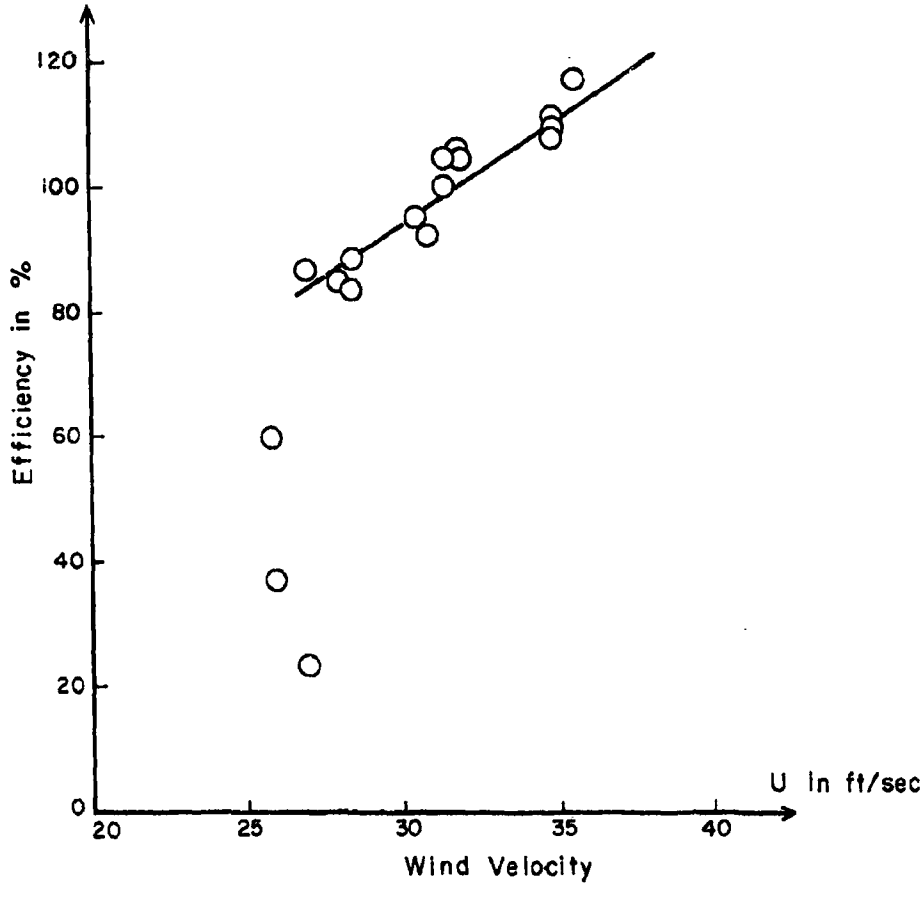

FIGURE 19 - EFFICIENCY OF THE VERTICAL TRAP

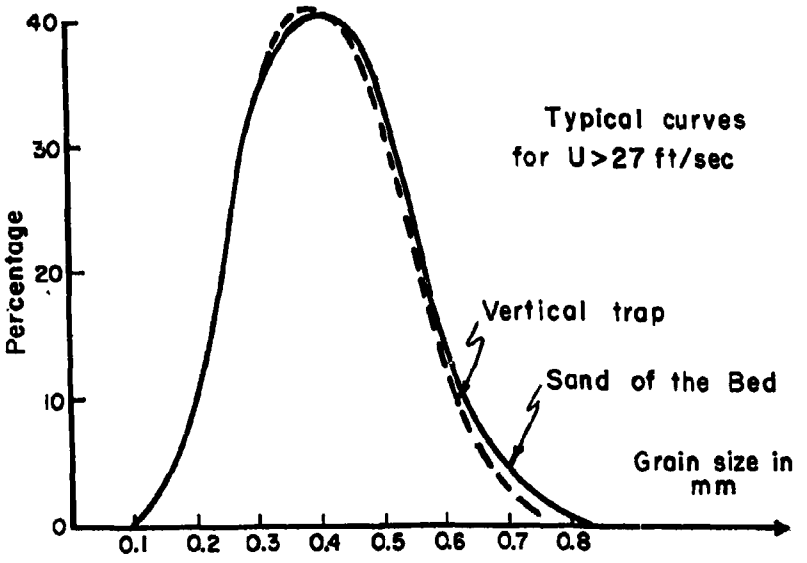

FIGURE 20 - GRAIN SIZE DISTRIBUTION FOR U>27 ft/sec

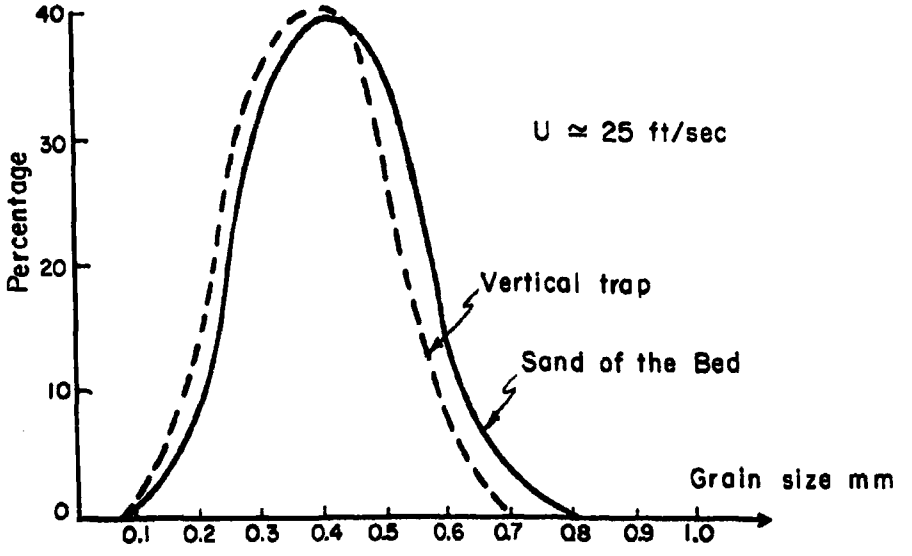

FIGURE 21 - GRAIN SIZE DISTRIBUTION FOR U≃25 ft/sec

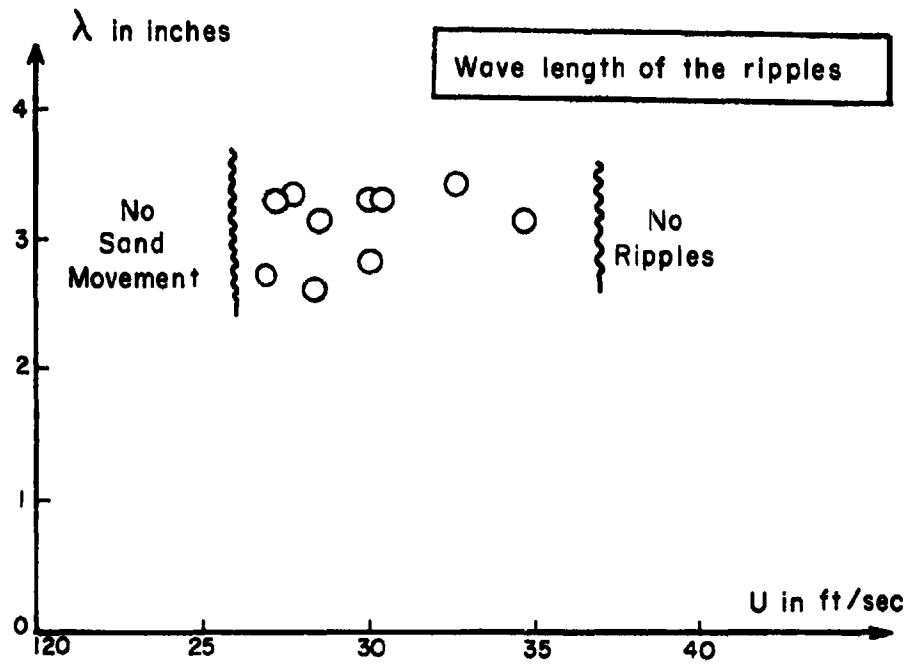

FIGURE 22 - WAVE LENGTH OF THE RIPPLES

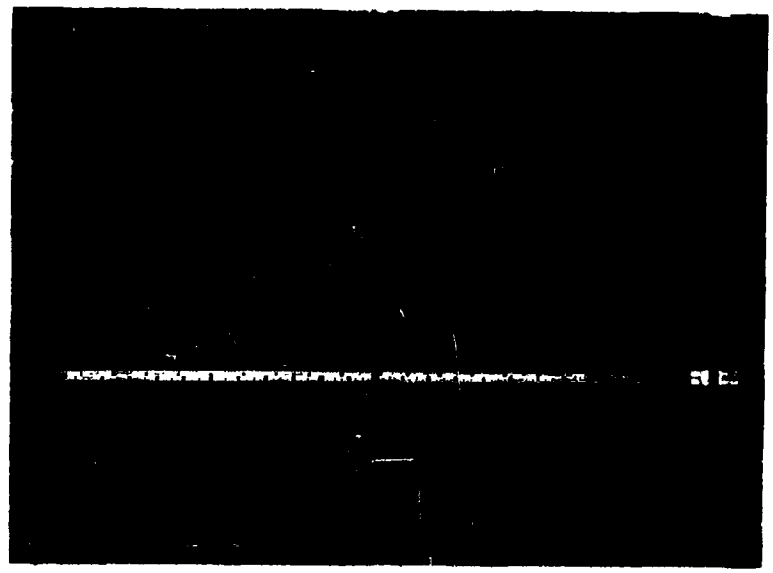

FIGURE 23- RIPPLES ON SAND SURFACE
U = 31 ft/sec
λ = 2.7 inches

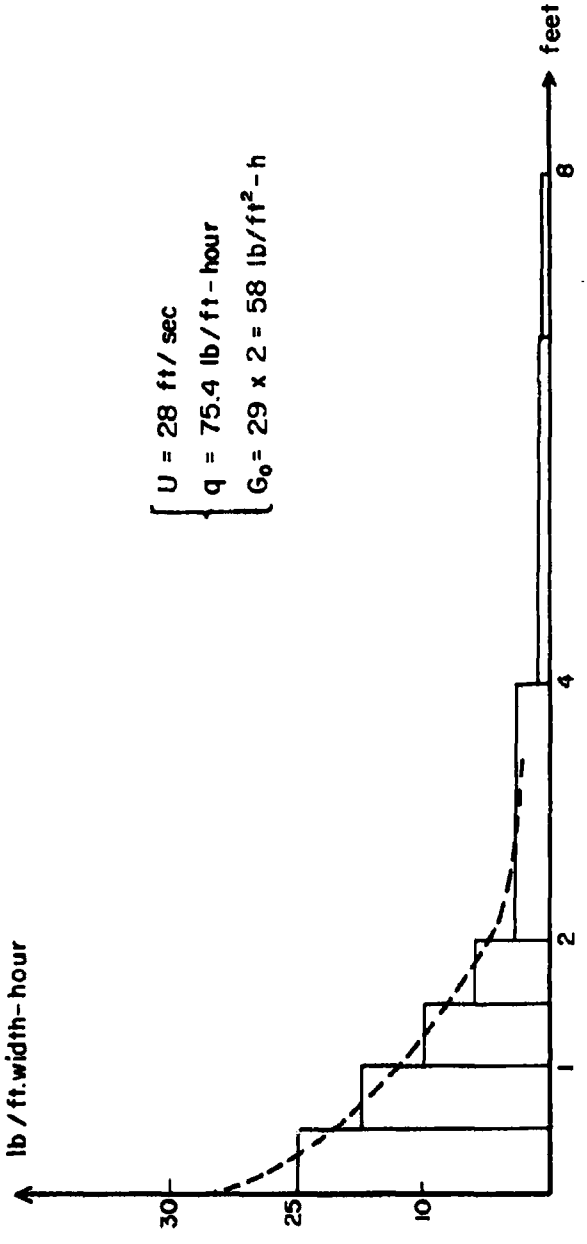

FIGURE 25- HORIZONTAL DISTRIBUTION OF SAND DRIFT

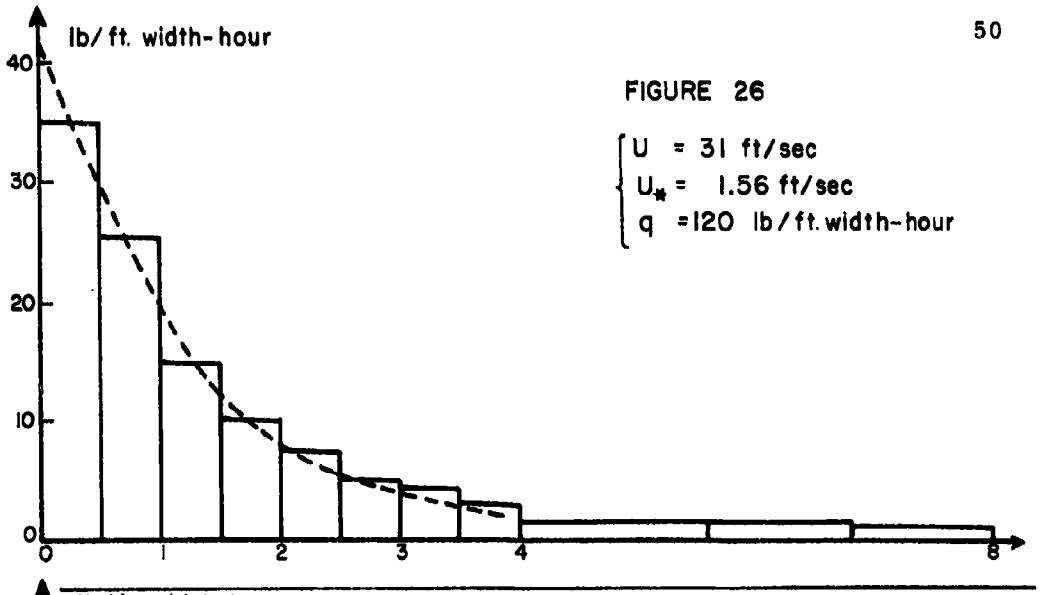

FIGURE 26

U = 31 ft/sec
U_* = 1.56 ft/sec
q = 120 lb/ft. width-hour

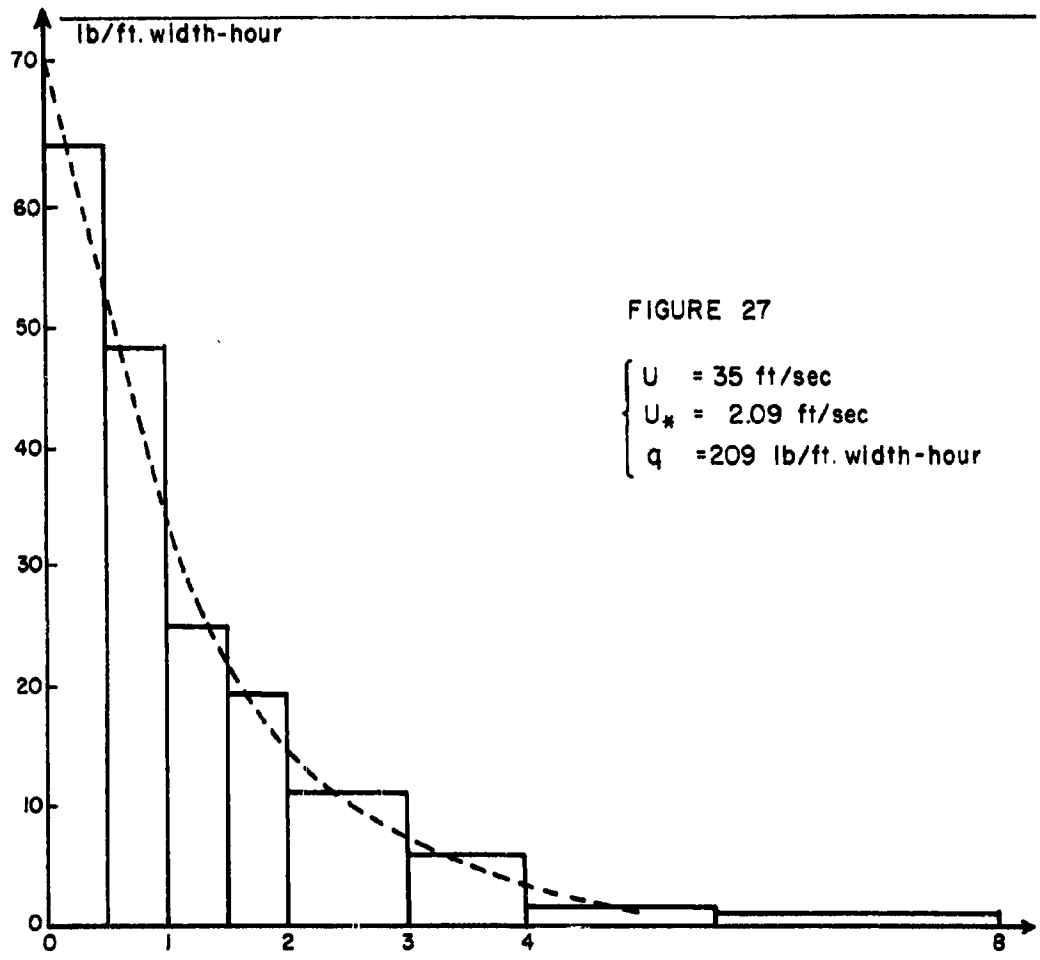

FIGURE 27

U = 35 ft/sec
U_* = 2.09 ft/sec
q = 209 lb/ft. width-hour

FIGURES 26, 27 - HORIZONTAL DISTRIBUTION OF SAND DRIFT

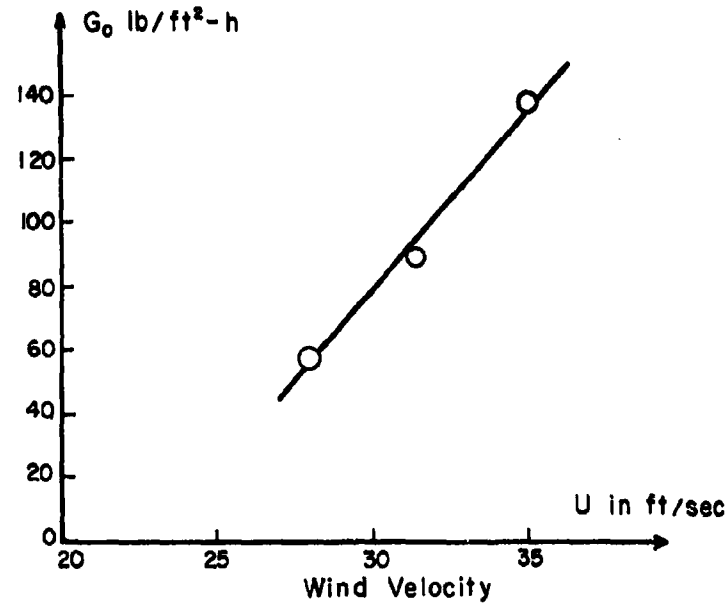

FIGURE 28 - AMOUNT OF SAND FALLING ON UNIT AREA OF SAND BED PER UNIT TIME, G_o

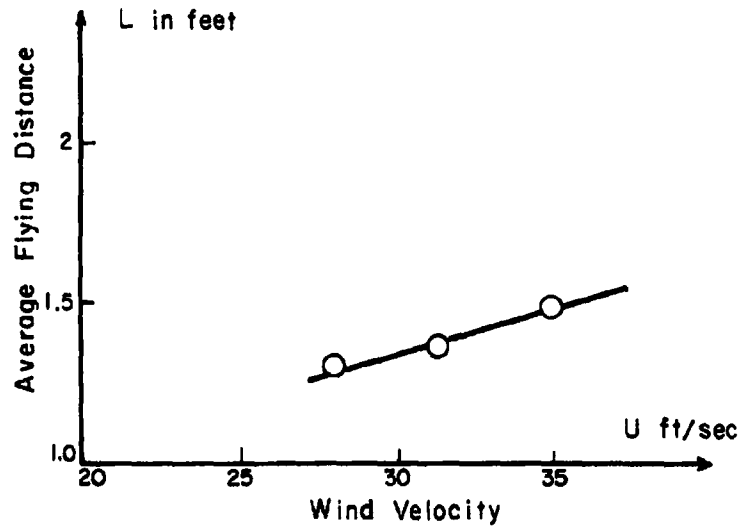

FIGURE 29 - AVERAGE FLYING DISTANCE

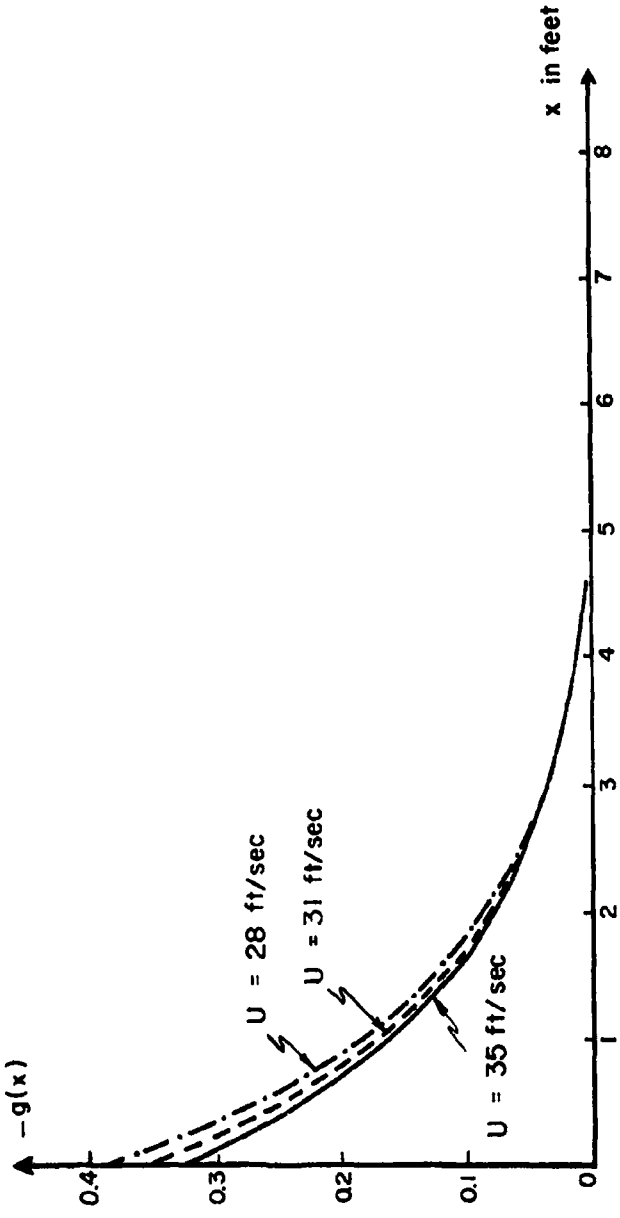

FIGURE 31 - FREQUENCY DISTRIBUTION FUNCTIONS OF FLYING LENGTH

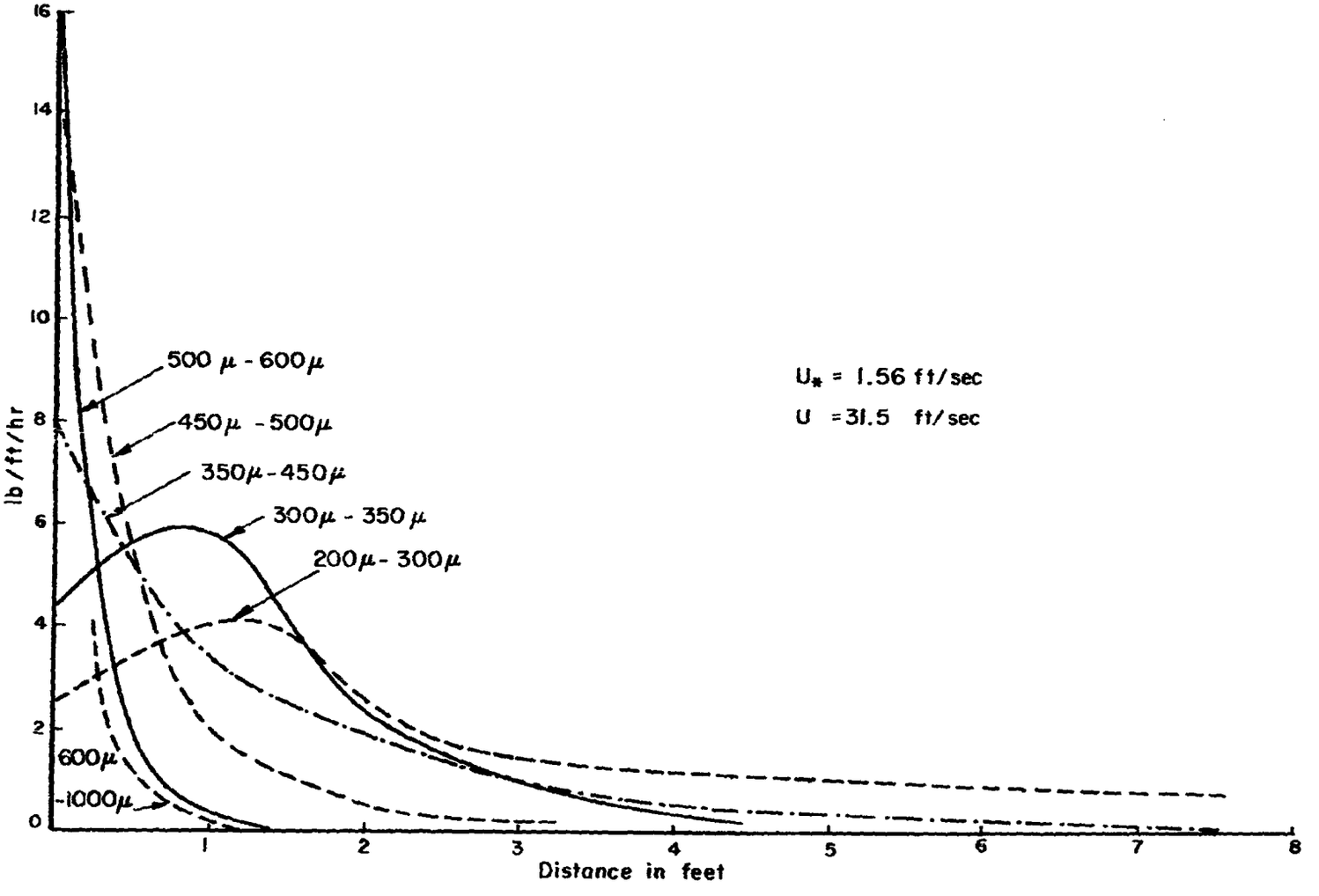

FIGURE 32 - SAND DISTRIBUTION IN THE HORIZONTAL TRAP FOR DIFFERENT GRAIN SIZES

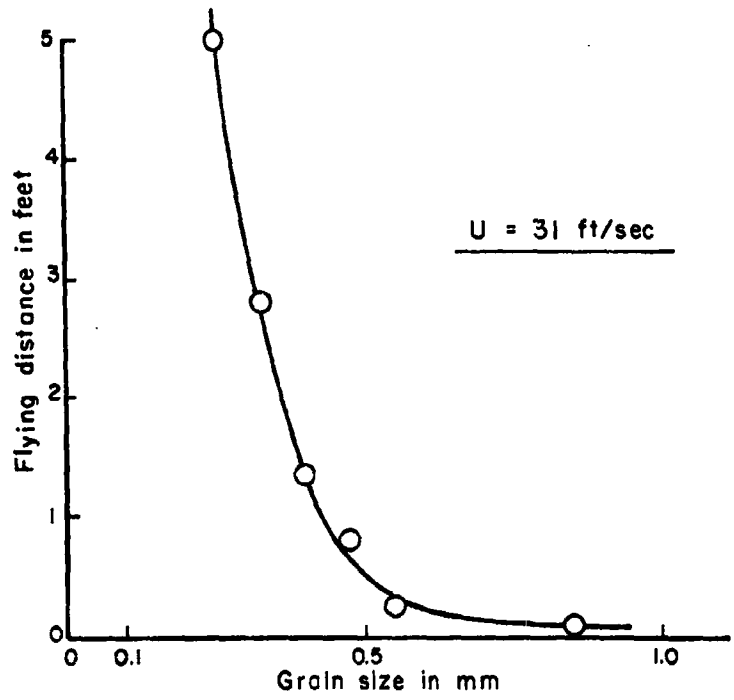

FIGURE 33- FLYING DISTANCE

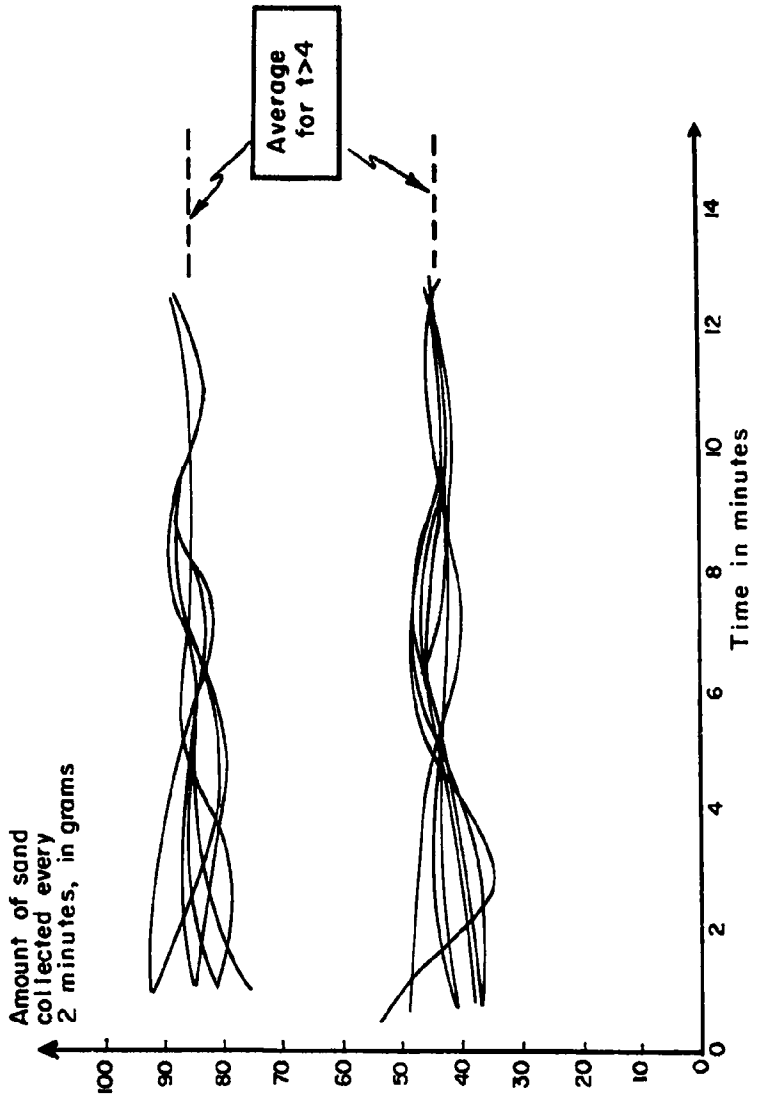

FIGURE 34

N.B. The average of all the values obtained on the amount of sand collected for a particular velocity, has been taken as a reference in plotting the discrepencies. This has been done in order to compare the magnitude of the discrepencies to the absolute values of the amount of sand collected, but has no quantitative value.

ADDENDUM I

STUDIES WITH 0.30 MM DIAMETER SAND

The section in the previous study dealing with the variation in the rate of sand transport and flying distance with the wind velocity has been repeated with a sand of smaller grain size.

The sand used in this new study had a mean diameter of 0.30 mm and a rather narrow range of grain sizes (Fig. 1).

The experimental procedure was exactly the same and U_* was again calculated by the formula:

$$U = 6.13\, U_* \log \frac{Z}{Z'} + U'$$

A sand feed-in was used in all runs, in order to create an artificial impact on the sand bed. This compensates for the size of the bed so that the results obtained approach those which would have been given by a sand bed of infinite length.

The threshold shear velocity (with sand feed-in), was 16 cm/sec. This value agrees fairly well with the value obtained from the Bagnold formula concerning the impact threshold:

$$U_{*t} = 0.09\sqrt{\left(\frac{\sigma - \rho}{\rho}\right) gd}$$

which gives

$$U_{*t} = 18 \text{ cm/sec for } d = 0.30 \text{ mm}.$$

The coordinates of the focal point were found to be:

$$Z' = 0.010 \text{ ft/sec}$$

$$U' = 9 \text{ ft/sec}$$

As for the sand used in original experiment (d = 0.44 mm), the focal point agrees quite well with Zingg's estimate of,

$$Z' = 0.092 \text{ ft}$$

$$U' = 8.8 \text{ ft/sec}$$

The rate of sand transport is plotted against the shear velocity in Fig. 2. This curve intersects the curve obtained with the 0.44 mm sand. This fact could have been theoretically foreseen, since according to Bagnold formulae:

$$U_{*t} = A \sqrt{\frac{\sigma - \rho}{\rho} gd}$$

$$q = \sqrt{\frac{d}{D}} \frac{\rho}{g} U_*^3$$

the threshold shear velocity U_{*t}, and the rate of sand transport, q, both increase with the grain size d.

Fig. 3 was prepared to present a comparison of the above data (Fig. 2) with the experimental results of Bagnold and Kawamura. The three curves differ considerably although the sand in each case had almost the same mean diameter. These variations might be explained by differences in the experimental equipment (length of the tunnel, presence

or absence of sand feed-in, and above all the length of the sand trap). Also the wind velocity distribution is sometimes difficult to define exactly, and the slightest deviation in its slope greatly influences the calculated value of U_* .

In the study with the sand of 0.44 mm diameter the Bagnold and Kawamura formulae could be used to describe the experimental data. However, in the present case it was impossible to find a constant in these formulae which would permit an adequate description of the experimental data. Figures 4 and 5 show the best description which could be obtained. The explanation of this fact was found by plotting the experimental data on log-log paper (Fig. 6). The data follow along a straight line the slope of which is about 2.8 instead of 3 as theoretically found by Bagnold and Kawamura. A similar disagreement had been already noticed by Horikawa, but the difference is too small in this case to question the theoretical formulae. In fact the slight disagreement which appears mostly for higher values of the wind velocity could be due to the unmeasured amount of sand transported in suspension by the wind: the amount of sand in suspension probably is not negligible for such a fine sand at the high velocities.

Figure 7 shows a typical horizontal distribution of sand in the horizontal trap. This curve can be used to calculate the average flying distance of the sand particles. For $U_* = 40$ cm/sec, the average flying distance, L, equals 9 inches which is much higher than the values obtained by previous investigators which are generally about 2 inches.

no clear explanation could be suggested for this discrepancy, but the shortness of the traps used by Bagnold, Kawamura and Horikawa might be a source of error in their findings. Also the possible presence of large scale turbulence above the traps might invalidate the present results.

Conclusions

This additional study for the smaller grain size has simply confirmed the conclusions of the original experiments on the larger grain size.

The theoretical aspect of the subject does not seem to pose any problem, but further study is needed to explain the discrepancies in the experimental data obtained by the various investigators concerning the rate of sand transport and the flying distance of the particles.

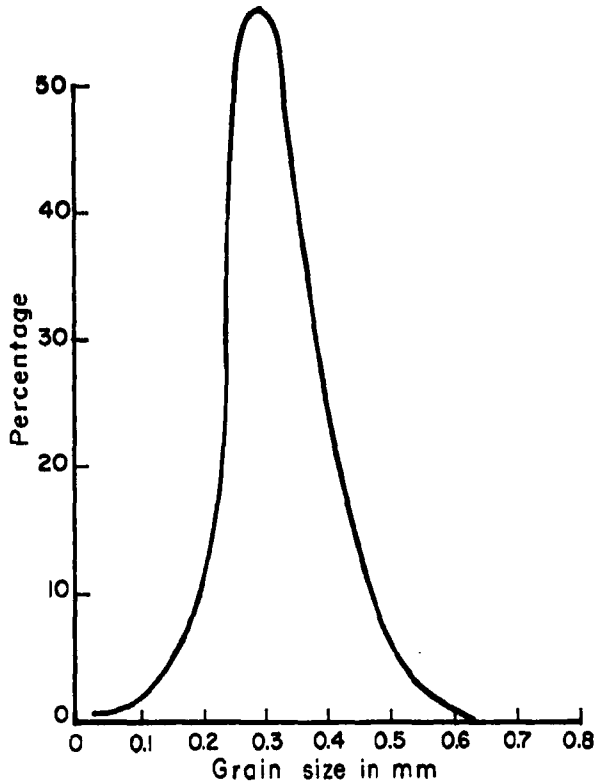

FIGURE 1 - GRAIN SIZE DISTRIBUTION

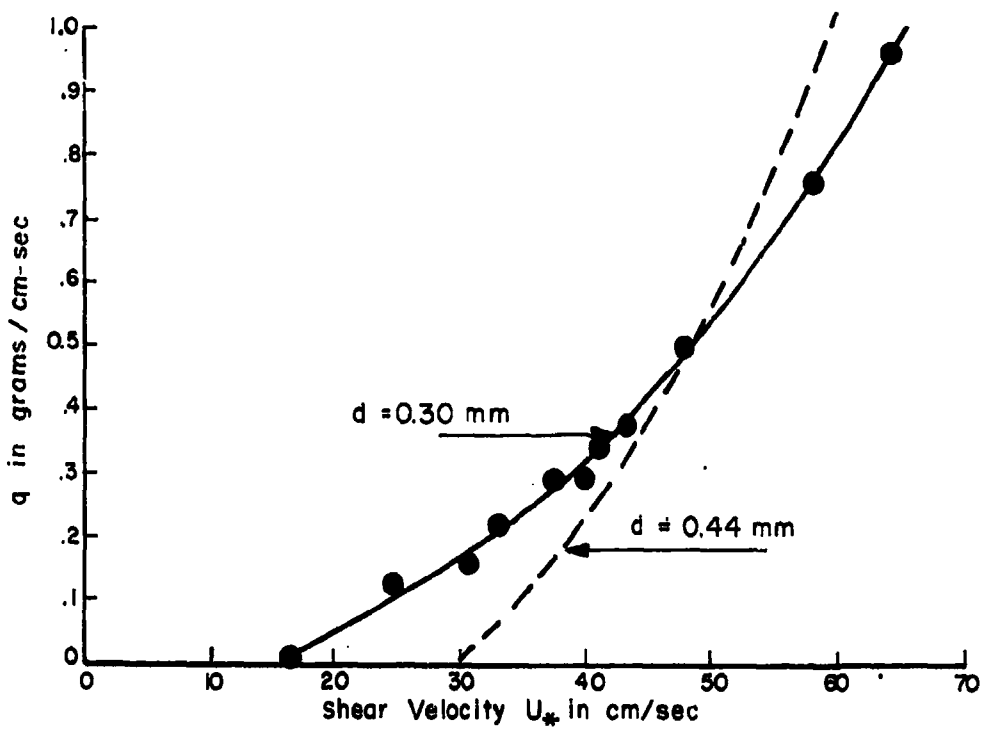

H8695A

FIGURE 2 - RATE OF SAND TRANSPORT

FIGURES 1, 2

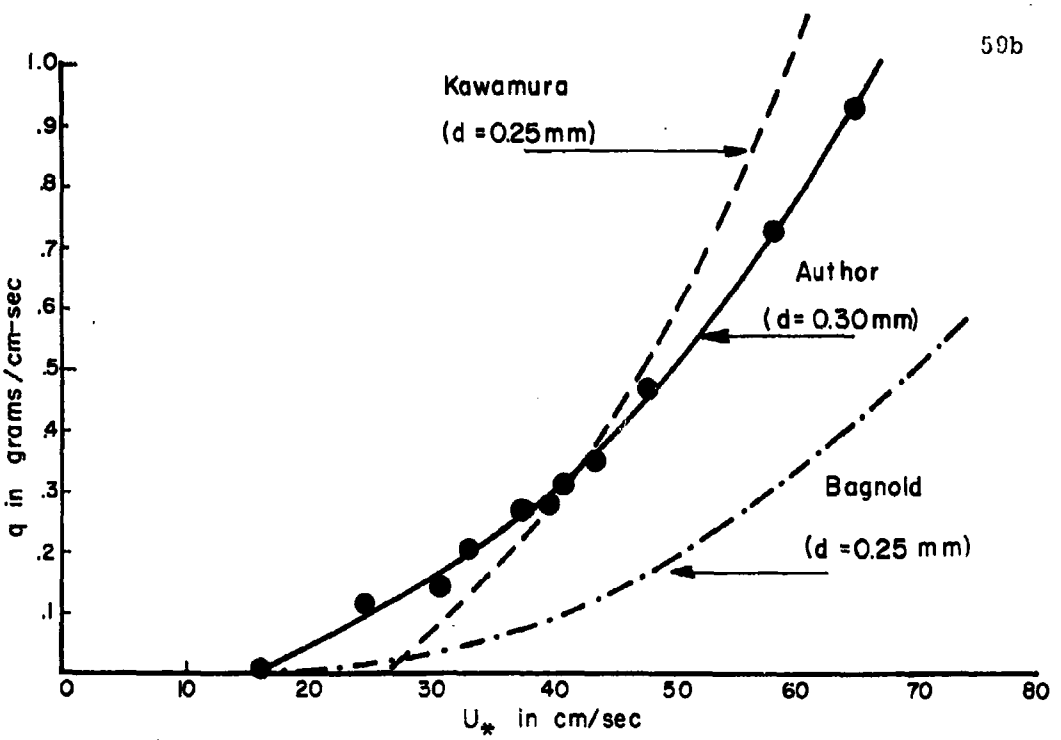

FIGURE 3 - RATE OF SAND TRANSPORT

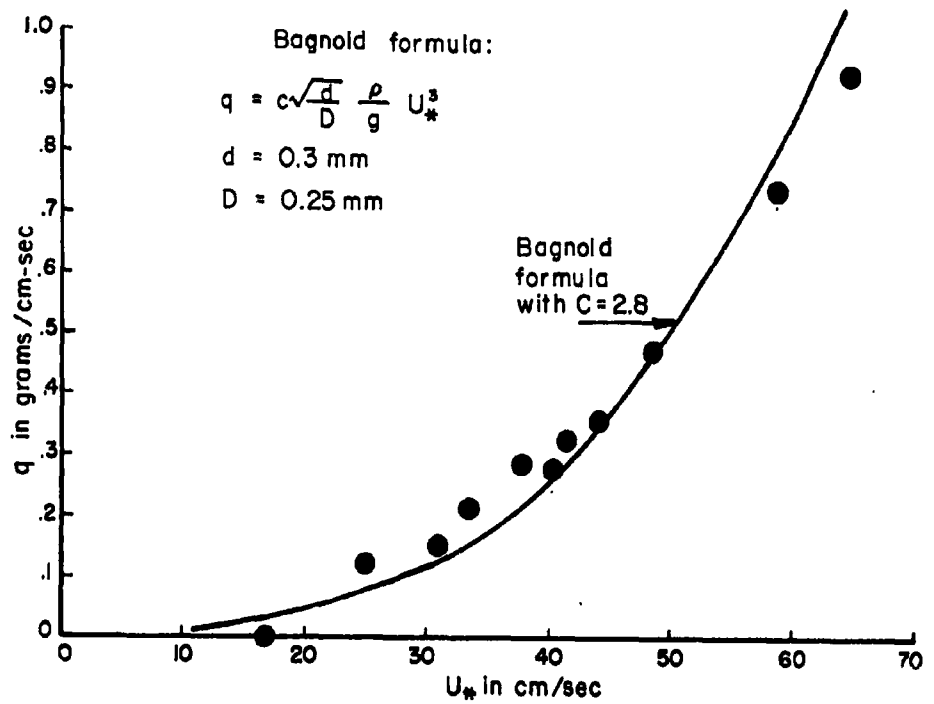

FIGURE 4 - COMPARISON BETWEEN EXPERIMENTAL RESULTS AND BAGNOLD FORMULA

H8696 A

FIGURE 3, 4

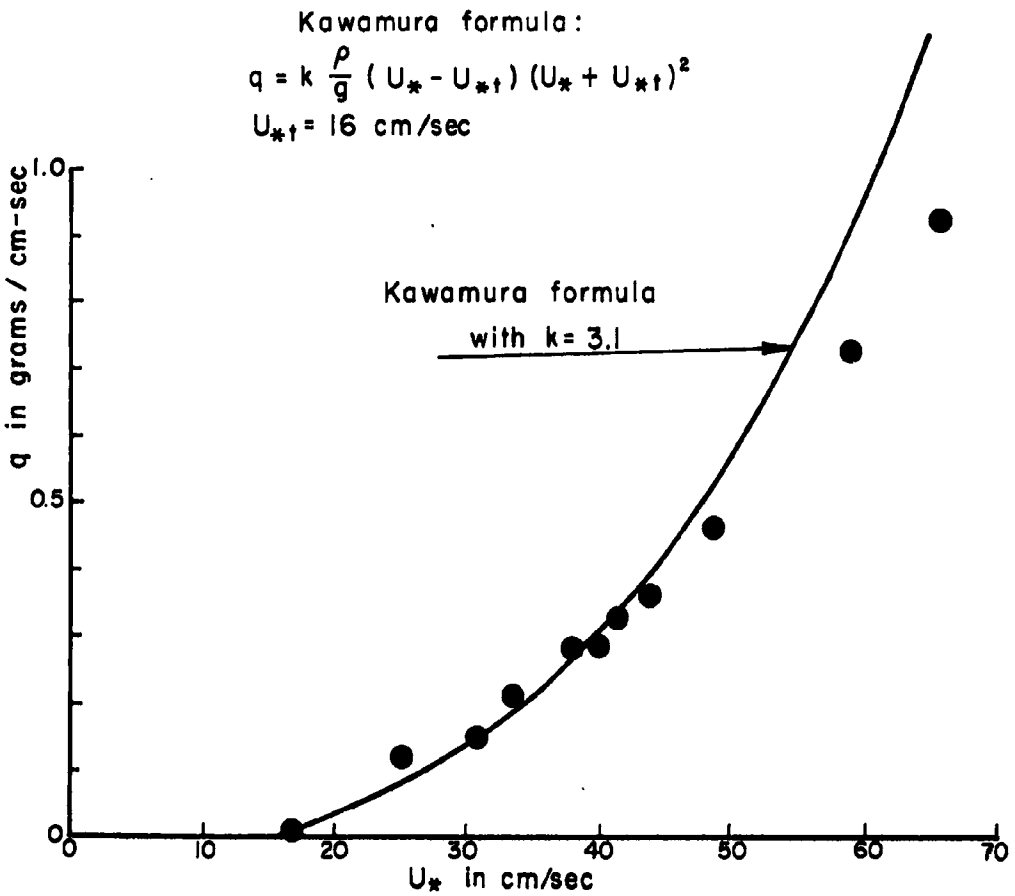

FIGURE 5-COMPARISON BETWEEN EXPERIMENTAL RESULTS AND KAWAMURA FORMULA

H 8897A

FIGURE 5

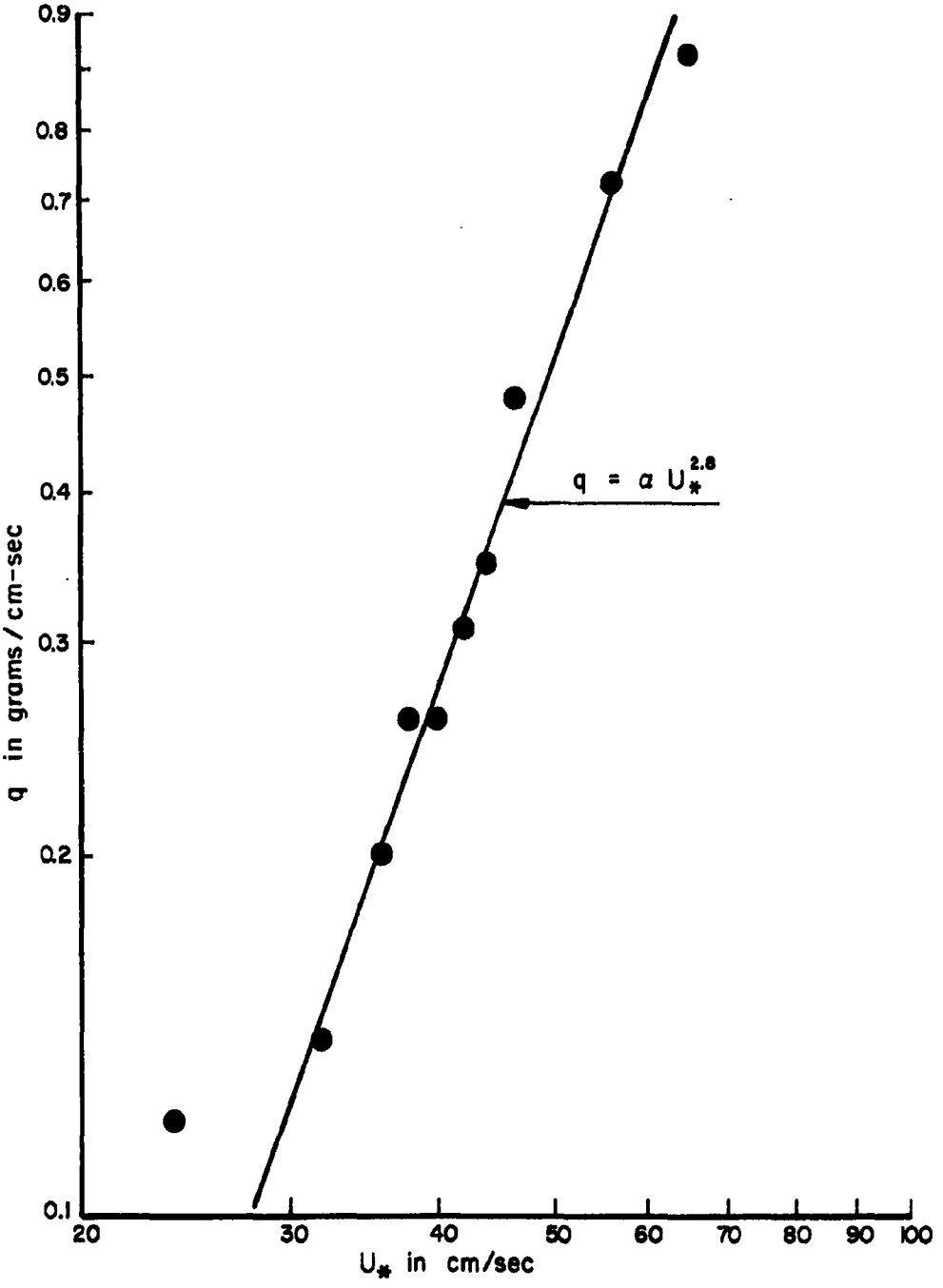

FIGURE 6- RATE OF SAND TRANSPORT

H 8898 A

FIGURE 6

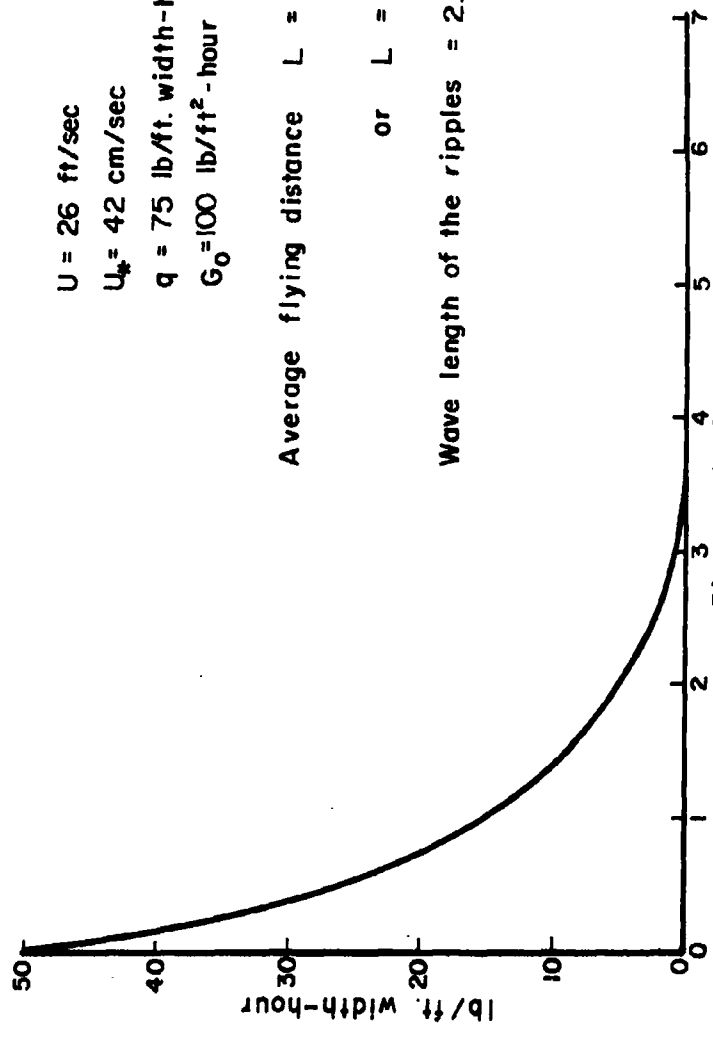

FIGURE 7 - TYPICAL HORIZONTAL DISTRIBUTION OF SAND DRIFT

H 8899 A

FIGURE 7

ADDENDUM II

INFLUENCE OF MOISTURE ON THE THRESHOLD OF SAND MOVEMENT

INTRODUCTION

When a flow of air over a flat bed of loose grains is gradually increased, there comes a certain moment when the sand grains are put into motion by the force of the wind (which can be measured in terms of shear velocity U_*). This critical value of the wind velocity is called the threshold velocity, and the corresponding value of the shear velocity, the threshold shear velocity is U_{*t}. This threshold velocity depends mainly upon the characteristics of the sand and of its surface.

This subject has been investigated by many authors; among them, Jorissen[1], Jeffreys[2], Chepil[3], Zingg[4], but chiefly by Bagnold[7,8,9] in the particular case of sand.

1. Fluid and Impact Threshold

The fluid threshold is the critical value of the wind velocity which has to be reached in order to initiate movement in the hypothetical case of an extremely flat sand surface. The movement of the sand grains in this case is caused only by the drag of the wind.

The impact threshold, on the other hand, occurs when the sand is kept disturbed by the "impact" of oncoming grains upon it. It is the impact threshold which is generally observed under natural conditions, for there is always a temporary stronger wind or some irregularities of

the bed (pebbles, small mounds) which disturb the flow and increase the velocity locally. Both cause a local or temporary sand transport. The impact of grains already in motion on immobile sand helps the wind drag to put the latter into motion; and this process repeats itself. After a short time, the sand movement extends over the entire surface. Thus, a continuous saltation of grains can be maintained for an indefinite distance downstream by a wind of feebler strength than the fluid threshold. The threshold wind strength at which this occurs marks the critical stage at which the energy supplied to the saltating grains by the wind just balances the energy losses due to friction when grains strike the bed.

2. Impact and Fluid Threshold for Uniform Sand

As a large-scale phemonom, the wind over an open dune, and the air flow in a wind tunnel (at a distance from the tunnel entrance for an open-circuit type tunnel) can be considered as fully turbulent. Dealing now with small-scale flow over and around the individual grains on the surface, the Reynold's number characterizing the flow is,

$$\frac{U_* d}{\nu}$$

where U_* is the shear velocity, d the mean size of the surface roughness (which is of the same order as the grain diameter), and ν the kinematic viscosity of the fluid (0.14 for air in c.g.s.units).

If $\frac{U_* d}{\nu} > 3.5$, the surface is rough and the threshold shear velocity which must be attained by the fluid before it can move any surface grains varies, as shown by Bagnold, as the square root of the grain diameter, according to the equation,

$$U_{*t} = A\sqrt{\frac{\sigma - \rho}{\rho} g d}$$

where σ is the density of the grain material and ρ is the density of air. A is a coefficient which equals 0.1 in the case of the fluid threshold. Since the impact threshold is lower than the fluid threshold, the coefficient A will be slightly smaller, and approximates the value of 0.08.

For smaller grains, when $\frac{U_* d}{\nu} < 3.5$, the surface approaches the smooth condition and the coefficient A is no longer constant but increases as the grains become smaller and smaller. Figure 1 gives the variations of Fluid and Impact Threshold with grain size as found by Bagnold.

3. The Fluid Threshold for Natural Sand

Usually the natural sand is a mixture in which one size of grain predominates, and in which the proportions by weight of grains of greater and smaller diameter decrease as the size departs from that of the predominant grains. If the material is well mixed and is spread out over the ground, the surface may be assumed to contain exposed grains in the proportions in which they exist in the body of the material. Most of the fine grains lie in crevices between the larger ones, and are screened by these from the drag of the wind. Apart from a very temporary movement on the part of the few most exposed fine grains for which the threshold velocity is smaller than for the mean diameter the initial threshold wind velocity is that corresponding to the predominant diameter.

If the wind is not increased above the initial fluid threshold

strength, sand movement goes on until the grains of the predominant and smaller sizes have all been carried away from the exposed surface, leaving only those of larger diameter. Then the motion ceases. By raising the wind velocity, a further temporary movement is produced, and so on. Finally the result is a sand bed covered by a surface layer containing all the largest grains which were present in the removed layers. If the wind strength is still further raised till the largest grains begin to move, the motion is no longer temporary, but goes on indefinitely. This ultimate threshold is that corresponding to the largest grains present in the bed.

Since the wind may drop before the ultimate threshold is reached, the sand may be left in any state of surface arrangement and the wind strength required to move it again may be anything from the initial to the ultimate threshold. For normal sand, however, the biggest grains present are usually not more than twice the predominant diameter, so that the ultimate threshold is commonly exceeded, and the transient stages occur only over a small range of wind velocity.

4. The Impact Threshold for Natural Sand

Physically the impact threshold marks the critical stage at which the energy supplied to the saltating grains begins to balance the energy losses due to friction when the grains hit the bed. There appears therefore to be little direct connection between the impact threshold and the conditions at the surface which determine the fluid threshold. Bagnold found that for sand of mixed grain size the impact threshold is approxi-

mately that corresponding to the predominant diameter of the grains in surface creep.

PURPOSE OF THE EXPERIMENT

Measurements on sand movement, and particularly of the threshold velocity show a great scatter for both field and laboratory experiments. Wind velocity and grain size of the sand are certainly the major factors of sand movement, but due to the inherent complexity of the problem many other variables can play minor roles and could be responsible for the observed scatter. Below are summarized the possible factors:

- related to the wind	Temperature Humidity
- related to the sand	Structure Texture Moisture-Content
- related to the surface	Roughness Settlement Temperature

The moisture adsorbed by the sand holds its grains together. Evidence for this can be obtained from the different angles of repose of dry and wet sand. It is therefore easy to foresee that the moisture renders the extraction of the grains of a sand bed more difficult. The purpose of this experiment is to evaluate the general magnitude of this effect.

EXPERIMENTAL EQUIPMENT AND PROCEDURE

1. The Wind-Tunnel

In order to study the threshold of sand movement for different air humidities it is preferable to use a closed-circuit type wind-tunnel. Contrary to the open-circuit type, such a tunnel does not, at least in principle, require a constant addition of water vapor.

In order to simulate full-scale sand movement in a tunnel it is necessary that the air stream have a velocity magnitude and distribution and turbulence structure similar to those of natural wind near the ground, and that the working section be large enough to minimize wall-interference.

For the particular study of the fluid threshold of sand movement the bed should be limited in length, and no sand enter from above the up-wind extremity of the bed, because only in such a condition can the true fluid threshold be examined as distinct from the impact threshold.

A wind tunnel located in Building 160 at the University of California Richmond Field Station fulfilled the above conditions and was used in the present experiment. The elevation and plan of this tunnel is shown in Fig. 2. The working section is on the suction side of the fan and is shown in Fig. 3 with a sand bed ready for testing. This chamber is 1 ft high, 2 ft wide and 3 ft long. One side was made of plastic to permit visual observations during tests.

The motor operating the fan was always set at a constant rotational speed. A wind speed range of 17 to 43 ft/sec could be obtained by con-

trolling a sliding valve placed on the exhaust side of the fan.

The sand was placed in a box, 2 inches deep and 25 inches long, which could be removed from the working chamber. The surface of the sand was brought to a height equal to that of the upwind and downwind floor of the tunnel.

Since the experiments were never conducted for high rates of sand transport, most of the blown-off sand could be collected in a sand trap, 2 inches long, placed immediately downwind of the end of the sand bed. The sand which was not caught in this trap was deposited in the vicinity of the valve, so that the air was free of sand particles when arriving again in the working section.

2. Wind Velocities Measurements

It is essential when measuring the velocity gradient at which the fluid begins to cause sand movement that a sufficient length of sand surface exist up-wind of the point of measurement, so that the fluid may have an opportunity to adjust the velocity distribution appropriate to the texture of the sand bed. Otherwise, except at levels immeasurably close to the surface, the velocity distribution will be that of the smooth floor further up-wind.

Wind velocities were measured with a standard Prandtl type pitot tube which was attached to a point gage and introduced into the air stream through the top of the flume. In order that the velocity distribution adjust to the sand bed the pitot tube was placed along a vertical which was almost at the end of the sand bed. The pitot tube was connected to an

Ellison type draft gage having a range of one inch of water and graduated into division of 0.01 inches. The pitot tube had a "coefficient" of 1. The wind velocities therefore were calculated by the formula,

$$U = \sqrt{\frac{2pg}{\rho}}$$

where p is the differential pressure at the pitot tube, and ρ the density of air, and g the acceleration of gravity. Atmospheric pressure, air humidity and air temperature were taken into account in determining the air density.

3. Sand Dampening

In order to study the movement of moist sand by wind, during a preliminary trial, the sand was dempened by spraying some water on its surface and a wind of normal humidity was allowed to blow through the tunnel. It was immediately noted that this method was inappropriate because the wind dried the surface layer of the sand bed invalidating the results. Thus the following procedure was adopted:

1) Study the movement of sand by winds of various humidities. The wind was allowed to blow over the sand for a sufficiently long time to dampen the sand surface.

2) Study the movement of sand by wind for higher water content of the sand, by adding water directly to the sand. In this case it was necessary to have the wind saturated with water, so that the surface layer of the sand does not dry quickly.

There are several methods of measuring the moisture content of

a soil. Among them are electrical methods (generally based on resistivity measurements) and radioactive methods. They all require more or less complicated equipment, and they all have to be calibrated with reference to the direct method consisting of weighing samples before and after drying. They are therefore less accurate than the direct method. The direct method is generally not feasible because of the time element involved. As an oven was made available by the Sanitary Engineering Laboratory of the University, and since time was not a controlling factor, the direct method was therefore used.

Sampling was done inside the tunnel and sample boxes were immediately sealed (also inside the tunnel in order to retain in the box the air of the tunnel). The samples were then taken to the Sanitary Engineering Laboratory, weighed (using a balance sensitive to a 1/100 of a gram) and then placed in an oven at 105° Centigrade. Twenty-four hours later the sample containers were again weighed and the water content, w, calculated as,

$$w \text{ in } \% = \frac{\text{Wet weight - dry weight}}{\text{dry weight}} \times 100$$

4. Humidification of Air

Water vapor was added to the air inside the tunnel by using a pan of water heated by 3 submerged 666 watt electric heaters. The free surface of the water had an area of about 3 ft^2. While heating the water, the fan was used from time to time to help circulate the air in order to obtain a homogeneous mixture of water vapor and air.

The air humidity is defined as,

$$h = \frac{\text{amount of water vapor present}}{\text{amount of water vapor for saturation}}$$

and was determined by using a wet and dry bulb thermometer and tables published by the U. S. Weather Bureau[5]. The apparatus was placed in the working section and the wet bulb had the museline wick dipped in water to keep it constantly wet.

It was very difficult to keep the air at a particular humidity during tests, because the water vapor condensed on the wall of the tunnel and around the fan when air is circulating in the tunnel. Thus, as much as possible, the experiments were conducted with air at its normal humidity. The natural variations in air humidity (45 to 70%) were sufficiently large to give significant results. The artificial humidification was used to experiment with air of humidity approaching saturation and in this case the air humidity was taken as the average between the measurements made at the beginning and at the end of each run.

5. Measurement of the Threshold

A natural sand having a mean diameter of 0.44 mm was used in this study. This sand had a relatively wide range of grain sizes as can be seen in Fig. 4. As already noted the threshold will therefore occupy a relatively wide range of wind velocities. It was decided to take account only of the "ultimate threshold", i.e., the lowest wind strength which gives a general movement of the sand. This choice was dictated by the following considerations:

(a) - the ultimate threshold has more significance than the initial threshold as far as natural conditions are concerned. It is the lowest value of the wind strength which gives a measurable sand-removal.

(b) - the value of the ultimate threshold does not depend on the past-history of the sand bed as is the case for the initial threshold, since for the former, grains of all diameters can be moved by the wind.

(c) - the wind velocity measurements are easier to make because the state of ultimate threshold lasts indefinitely, whereas the initial threshold lasts only as long as the grains of the predominant diameter are present on the surface layer.

The accurate definition of the ultimate threshold is, however, a difficult matter. Thus, instead of a visual observation, the threshold was defined as occurring when the rate of sand caught in a small trap beyond the end of the sand bed had a certain value (0.04 gram/cm-sec). When this rate had not been obtained directly, an interpolation or extrapolation method was used.

EXPERIMENTAL RESULTS AND DISCUSSION

1. Preliminary Remarks

Besides supplying water to the sand, air humidity plays a role in the threshold problem by changing the ratio of the densities of sand particles and fluid. The Bagnold formula provides for this change in air density, that is,

$$U_{*t} = A\sqrt{\frac{\sigma-\rho}{\rho} g d} .$$

For a temperature of 70° F and a pressure of 30 inches of mercury, the completely dry air (h = 0%) has a density of 0.0755 lb/ft^3. For the same temperature and pressure, the air saturated with water (h = 100%) has a density of 0.0743. σ being much bigger than ρ, the above formula can be rewritten as,

$$U_{*t} \simeq A\sqrt{\frac{\sigma}{\rho} g d}$$

thus,

$$\frac{dU_{*t}}{U_{*t}} = -\frac{1}{2}\frac{d\rho}{\rho}$$

and for the above variation of ρ, the relative variation of U_{*t} is,

$$\frac{d U_{*t}}{U_{*t}} = -\frac{1}{2}\frac{d\rho}{\rho} = 0.7\%$$

This variation is so small in comparison with that which will be found

for actual variations, that the influence of humidity on air density can be neglected with respect to the role of sand moisture.

Moist sand found along coasts can be classified into two categories depending upon the origin of the moisture:

1) Moist sand which has collected moisture from the atmosphere. Unlike very fine particles such as dust or loess the sand does not readily absorb moisture. As proved later, there exists a correlation between the water content of the sand and air humidity. Allowing for this fact, and since in the field it is easier to measure the air humidity than the sand water-content, the air humidity instead of the water-content of the sand has been taken as the variable in this study.

2) Moist sand whose water comes from sources other than air humidity, such as: rain, rising of underground water, and sea water remaining in the sand by wave or tide action. When a wind not saturated with water vapor blows over such a sand, it gradually dries out the surface layer of the sand bed, until an equilibrium is reached between humidity of the wind and the water content of the surface layer of the ground. The study of sand movement in this case, where water contents of air and sand, as well as wind duration, come into play, is very complex. The first step in the solution of this problem consisted of studying the particular case of saturated wind blowing over a bed of moist sand (the water content of the sand being greater than that which could be obtained from air humidity alone) for only in this instance did the wind have no tendency to dry out the sand.

Therefore, the initial studies were on the threshold of sand movement for various air humidities and subsequently the threshold of sand movement when directly dampened with water, by a saturated wind. Finally an attempt at generalization was made by dropping the air humidity variable, and a relationship between the threshold and water-content of sand was developed.

2. Variation of the Threshold with Air Humidity

From a series of velocity distribution curves as given in Fig. 5, U_* was determined for different mean velocities and different air humidities. Figure 6 shows the relationship between the shear velocity, U_*, and the mean velocity, U. This relationship is quite consistent and can be expressed by a straight line. Thus, it can be said that the wind drag is practically uninfluenced by air humidity. In the later tests, only the value of the mean velocity was recorded and the value of U_* was calculated from this graph.

Since the wind velocity never exceeded the threshold value by an appreciable amount, it was very difficult to determine the elevation of the focal point of the velocity distributions (they are almost parallel), but its abscissa is probably about 20 ft/sec. This is somewhat more than the value of 13 ft/sec predicted from Zingg's formula[6]. The Zingg formula was well verified during previous experiments using the same sand but in a much longer tunnel*, so that the present difference may be due to the shortness of the bed which does not allow the wind to

* Ref.

reach an equilibrium profile. The water-content of sand obtained during the various runs is plotted against the corresponding air humidity in Fig. 7. The scatter is important, but there is a general tendency for the points to follow along a straight line (which obviously should pass through the origin).

As explained above, the threshold velocity was found by investigating the initial stage of curves for the rate of sand transport. The three sample curves in Fig. 8 clearly indicates the change in the rate of sand transport with humidity. From such curves the data on the variation of the threshold shear velocity distinctly show an increase with air humidity, and the relationship is nearly linear (Fig. 9). The few points which correspond to a threshold value manifestly lower than the average were probably obtained during runs in which the absorbtion of moisture by the sand had not reached its equilibrium value.

The increase of the threshold shear velocity with air humidity can be represented for the particular sand studied, by the equation

$$U_{*t} = 28\,(1 + \tfrac{1}{2}\,h/100)\ \text{cm/sce}$$

where 28 is the value given by the Bagnold formula for the threshold velocity in cm/sec, for the sand under investigation. Assuming a similar influence of humidity for sand of different grain sizes, the Bagnold formula can be modified as follows to provide for the air humidity factor.

$$U_{*t} = A\,(1 + \tfrac{1}{2}\ \ \tfrac{h}{100})\ \sqrt{\tfrac{\sigma - \rho}{\rho}\ g d}$$

where A is a coefficient whose value approximates 0.1 and h is expressed in percent.

3. Threshold for Sand of High Water-content

The maximum amount of water that can be imparted to sand by atmospheric humidity is 0.25%. For a water content greater than 0.25%, the relationship between U and U_* remains linear and seems, quite naturally, to be a prolongation of the previous curve, (Fig. 10).

During these runs the wind was constantly saturated and the water content of the sand, w, is now taken as the variable for the study of the threshold velocity. The results are summarized in Fig. 11. For a high water-content ($w > 1\%$) the wind strength necessary to initiate sand movement becomes more and more important. This increase could be explained by the fact that the sand surface becomes very smooth under wind action. The water contained in the sand fills up the interstices between the grains making the extraction of the grains by the wind much more difficult. The experiment could not be pursued for water-content higher than 4% because the wind strength necessary to initiate the movement could not be obtained with the equipment available; however, one would expect that the wind strength would increase very rapidly with an increase of water-content. It is even probable that for very high water-content (flooded sand) the problem changes aspect and becomes closer to the problem of an interface between two fluids.

Using the relationship between water-content and air humidity in Fig. 7, it is possible to complete the results of the study of low

water-content and thus find the relationship between U_{*t} and w for the total range of water content (0 to 4%). Figure 12 shows the curve obtained. As one would have expected, since the air humidity in itself does not play a role in the sand movement, there is no break at the point which joins the two sets of data. The curve suggesting an exponential function has been replotted on semi-log paper in Fig. 13. The data in these new coordinates appears to follow a straight line, thus indicating that the relationship between U_{*t} and w can be put into the form,

$$U_{*t} = a \log_{10} w + b$$

where a and b are two constants obtained from the graph. It was found that

$$U_{*t} = 17 \log_{10} w + 51 \quad \text{cm/sec}$$

or,

$$U_{*t} = 28 (0.6 \log_{10} w + 1.8) \quad \text{cm/sec}$$

where 28 is the value of U_{*t} in cm/sec given by the Bagnold formula.

These formulae or the graphs in Figures 12 and 13 summarize the results obtained in this study. Assuming that moisture affects the movement of sand of different grain sizes in the same manner, the Bagnold formula for the threshold shear velocity may be modified as follows,

$$U_{*t} = A\sqrt{\frac{\sigma - \rho}{\rho} g d} \quad (1.8 + 0.6 \log_{10} w)$$

where A approximates 0.1 and w is expressed in percent.

CONCLUSIONS

The experiments demonstrated that moisture clearly increases the value of the threshold shear velocity of sand movement. When the moisture has its origin in atmosphere humidity, the variation although a not negligible one, remains rather small for the usual range of air humidities. On the contrary when the water-content of the sand attains the values of 2 or 3% the wind strength necessary to initiate the movement becomes considerable.

If w is the water content expressed in percent, the threshold shear velocity U_{*t} is given by,

$$U_{*t} = A\ (1.8 + 0.6 \log w) \sqrt{\frac{\sigma - \rho}{\rho}\ g\ d}$$

When atmosphere is responsible for the sand moisture, it is preferable to use the formula,

$$U_{*t} = A\ (1 + \frac{1}{2}\ \frac{h}{100}) \sqrt{\frac{\sigma - \rho}{\rho}\ g\ d}$$

where h is the air humidity expressed in percent. In both formulae, d represents the mean grain diameter, σ and ρ are the density of sand grains and air, respectively, and A approximates the value of 0.1 for the fluid threshold and 0.08 for the impact threshold.

REFERENCES

1. Jorrissen, A., Sur le transport des particules solides. Mémoires de l'association des ingenieurs sortis de l'Ecole de Liege, No. 1, 1943.

2. Jeffreys, H., On the transport of sediment by streams, Proc. Cambridge Philosophic Society, Vol. 25, p 272, 1929.

3. Chepil, W. S., Dynamics of wind erosion, Soil Science
   Vol. 60, Oct. 1945, pp 305-320.
   Vol. 60, Nov. 1945, pp 397-411
   Vol. 60, Dec. 1945, pp 475-480

4. Zingg, A. W. and Chepil, W. S., Aerodynamics of wind erosion, Agricultural Engineering, Vol. 31, pp 274-284, June 1950.

5. Marvin, C. F., Psychrometric Tables, U. S. Department of Commerce, Weather Bureau, 1941.

6. Zingg, A. W., Wind tunnel studies of the movement of sedimentary material, Proc. of the Fifth Hydraulics Conference, pp 111-135, 1952.

7. Bagnold, R. A., The Physics of Blown Sand and Desert Dunes, Methuen & Co. Ltd., London, 1954.

8. Bagnold, R. A., The size grading of sand by wind, Proc. Royal Society of London, Series A, Vol. 163, No. 913, pp 250-264.

9. Bagnold, R. A., The movement of desert sand., Proc. of the Royal Society of London, Series A, No. 892, pp 594-619.

10. Malina, J., Recent development in the dynamics of wind erosion, Transactions of Amer. Geophysical Union, pp 262-284, 1941.

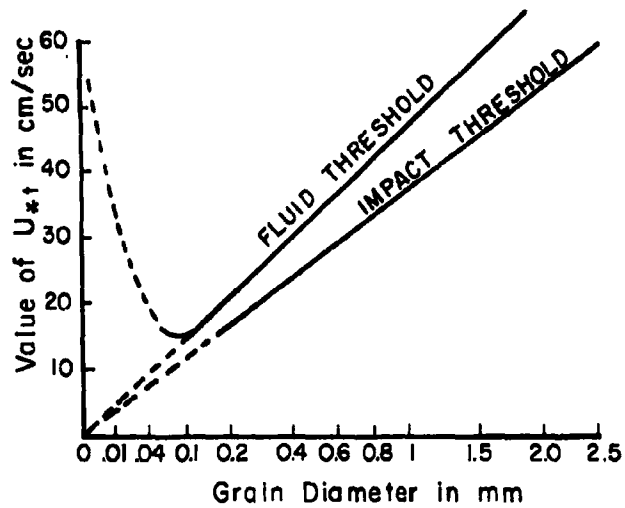

FIGURE 1 - VARIATION OF THE THRESHOLD WITH GRAIN SIZE

(after Bagnold)

H8818A

FIGURE 1

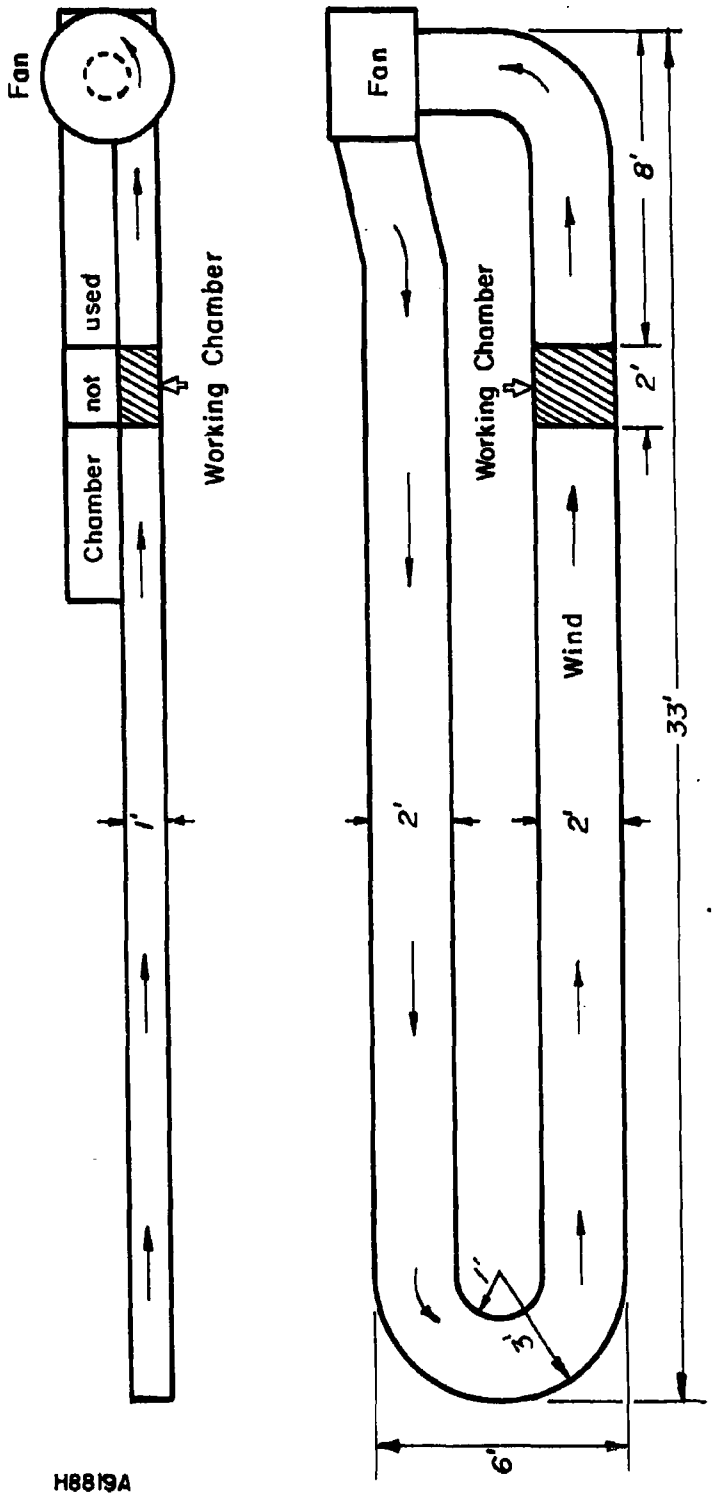

H8819A

FIGURE 2 - WIND TUNNEL

FIGURE 2

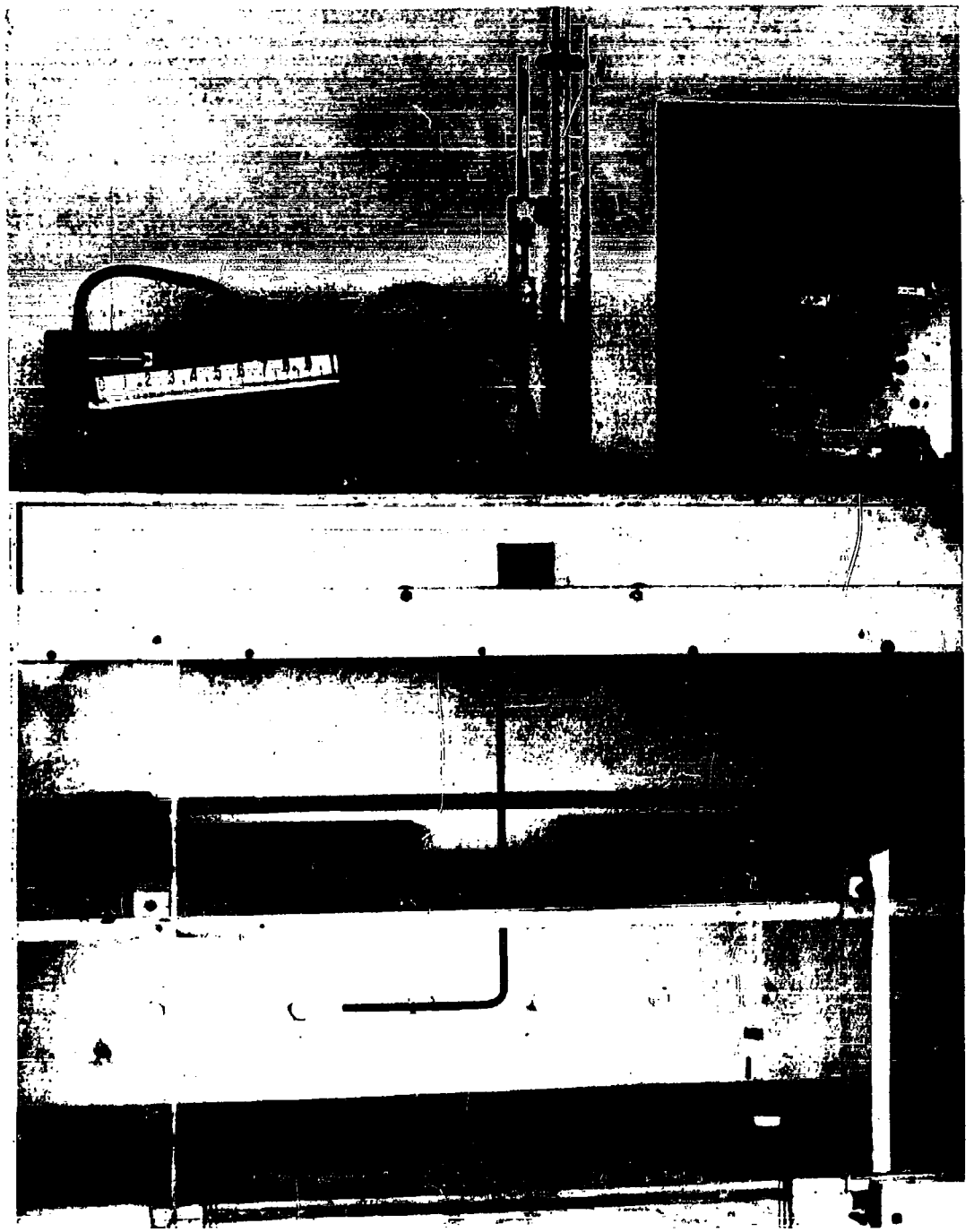

FIGURE 3 - THE WORKING CHAMBER. THE SAND BOX AND ITS TRAP ARE SHOWN BELOW, THE VELOCITY MEASURING EQUIPMENT, WET AND DRY THERMOMETER AND THE RHEOSTAT WHICH CONTROLS THE HEATERS ARE ABOVE.

H8820A

FIGURE 3

H8821A

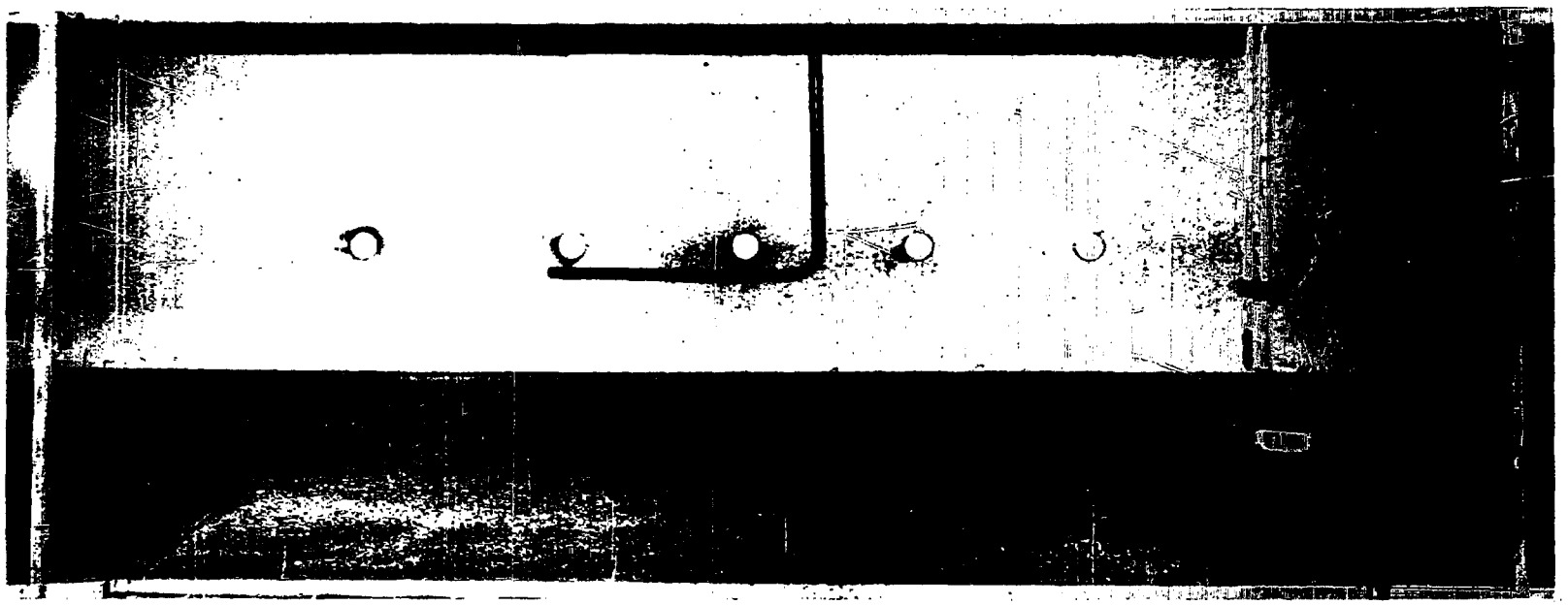

FIGURE 3a – CLOSE-UP OF THE WORKING CHAMBER

(This picture was taken during the preparatory stages. During the runs the location of the pitot tube was much further down-wind

FIGURE 3a

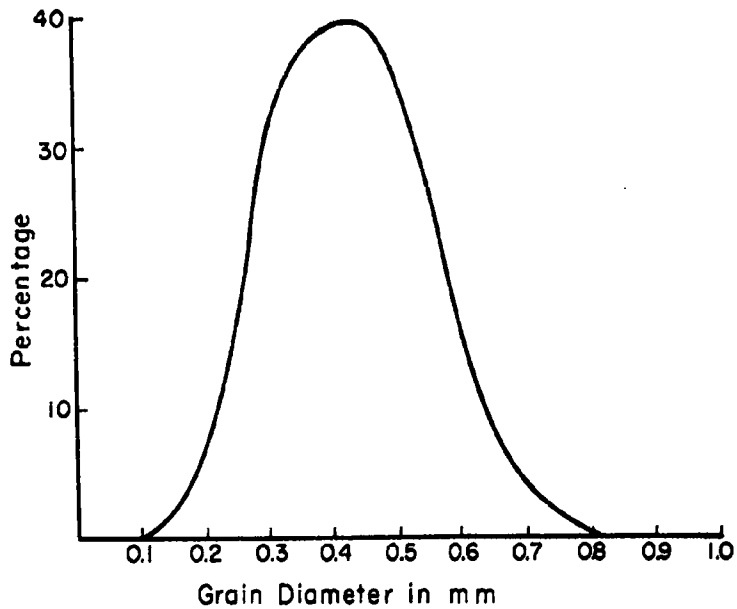

FIGURE 4 - GRAIN SIZE DISTRIBUTION

H8822A

FIGURE 4

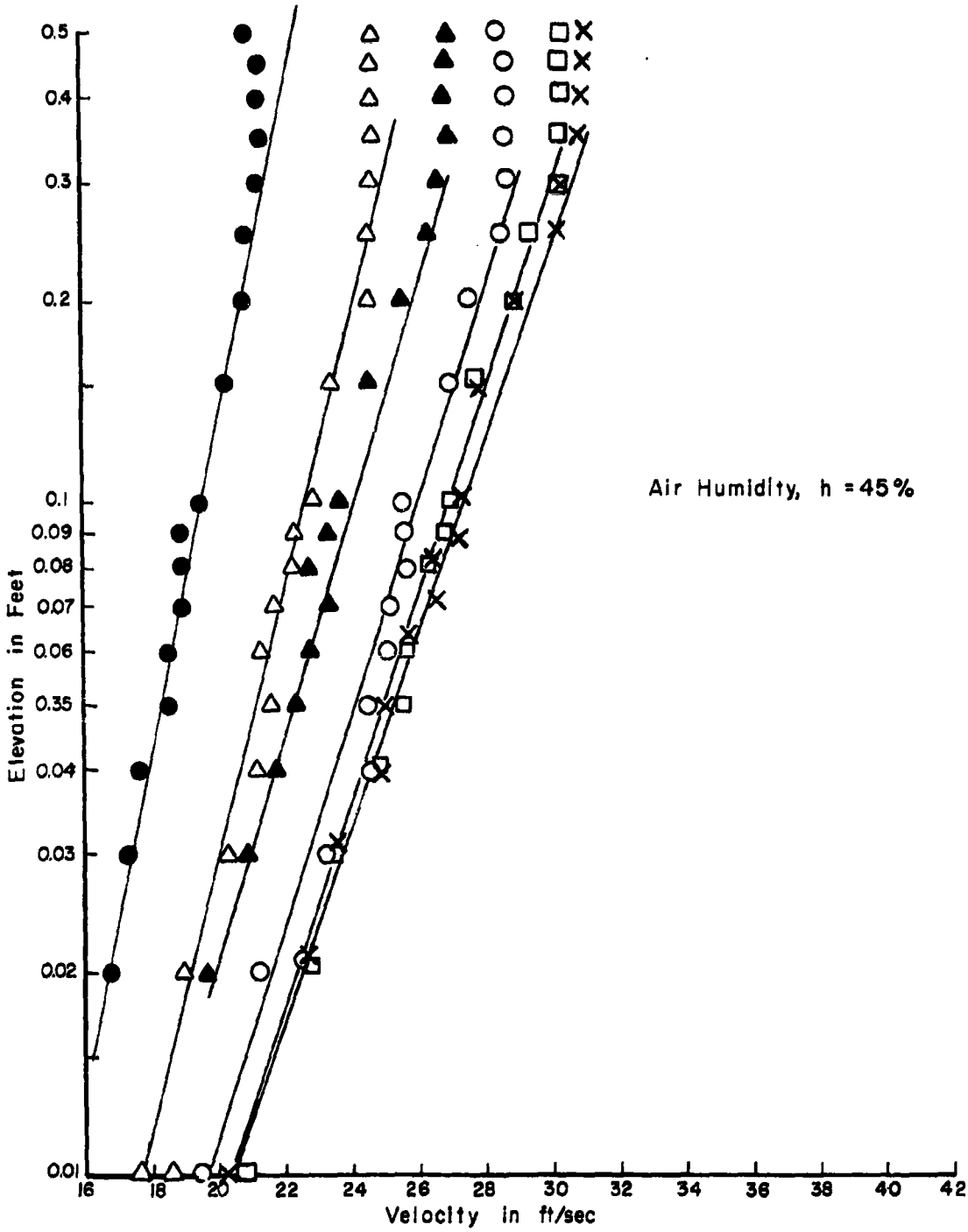

FIGURE 5 - TYPICAL VELOCITY DISTRIBUTION ABOVE SAND SURFACE

H8823A

FIGURE 5

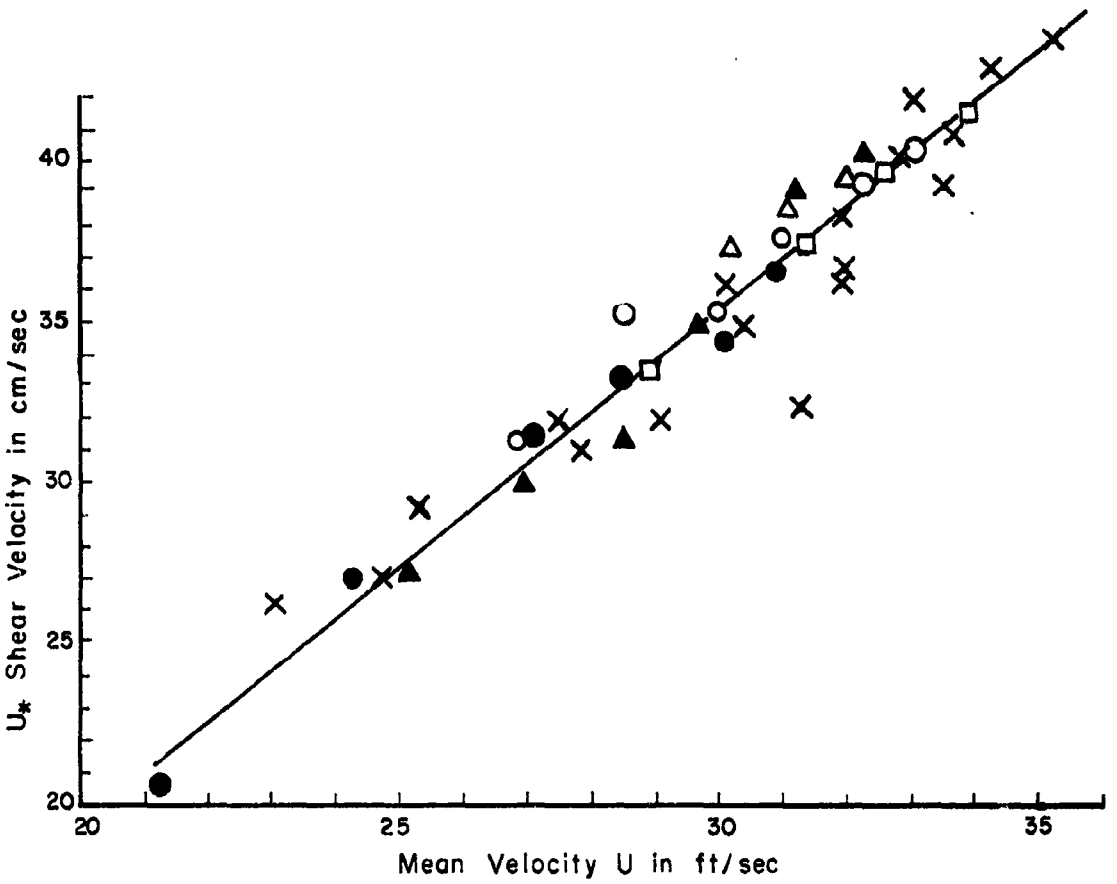

FIGURE 6 - RELATIONSHIP BETWEEN U AND U_* FOR DIFFERENT AIR HUMIDITIES

- ● h = 45 %
- ▲ h = 54 %
- ○ h = 57 %
- △ h = 68 %
- □ h = 73 %
- ✕ h = 100%

Note: The shear velocity U_* was calculated from the Prandtl equation with k = 0.40: $U_z = 5.75\ U_* \log \frac{z}{k}$

H 8824A

FIGURE 6

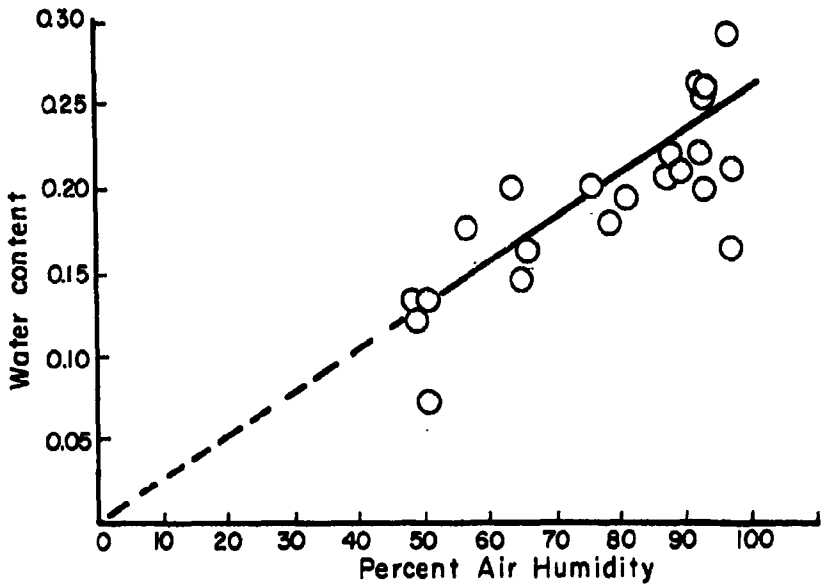

FIGURE 7 - RELATIONSHIP BETWEEN WATER CONTENT OF THE SAND AND AIR HUMIDITY

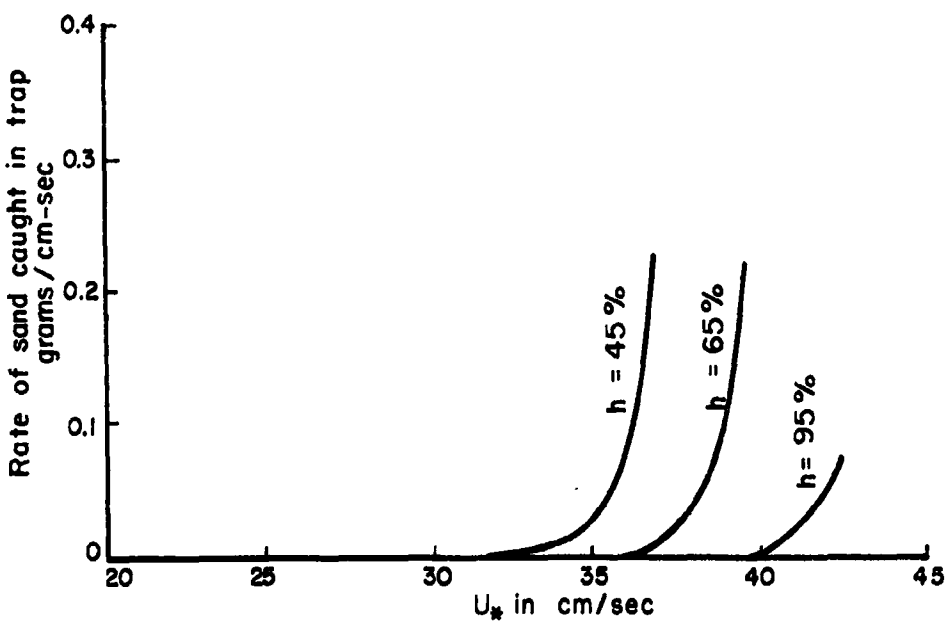

FIGURE 8 - VARIATION OF RATE OF TRANSPORT WITH AIR HUMIDITY

H8825A

FIGURES 7, 8

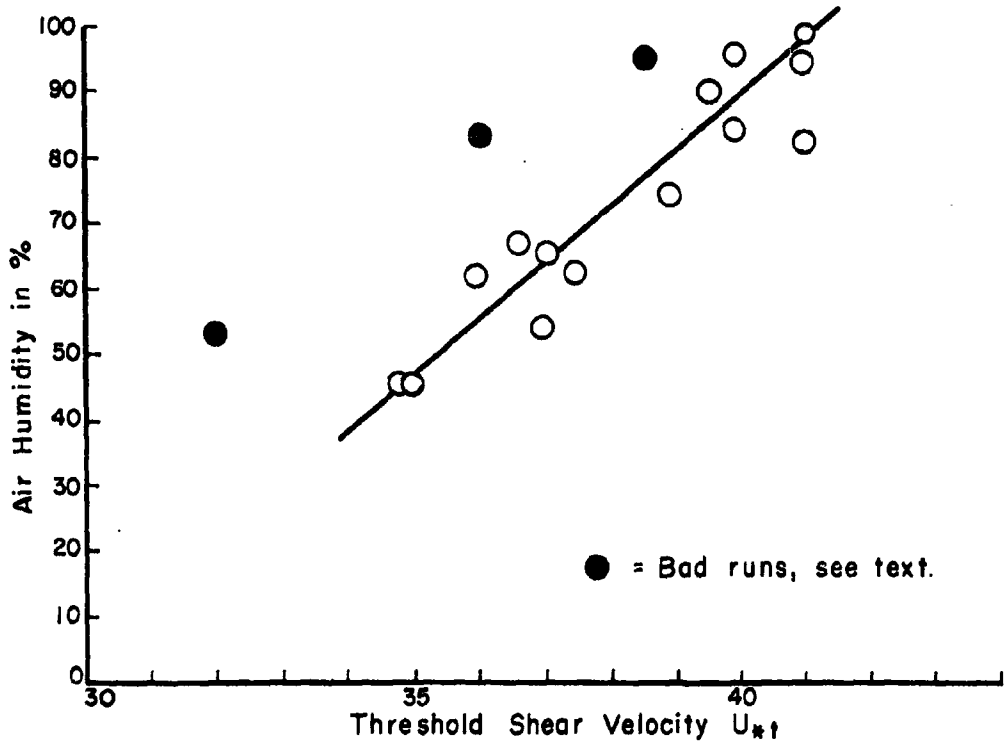

FIGURE 9- THRESHOLD VELOCITY AS A FUNCTION OF AIR HUMIDITY

H8826A

FIGURE 9

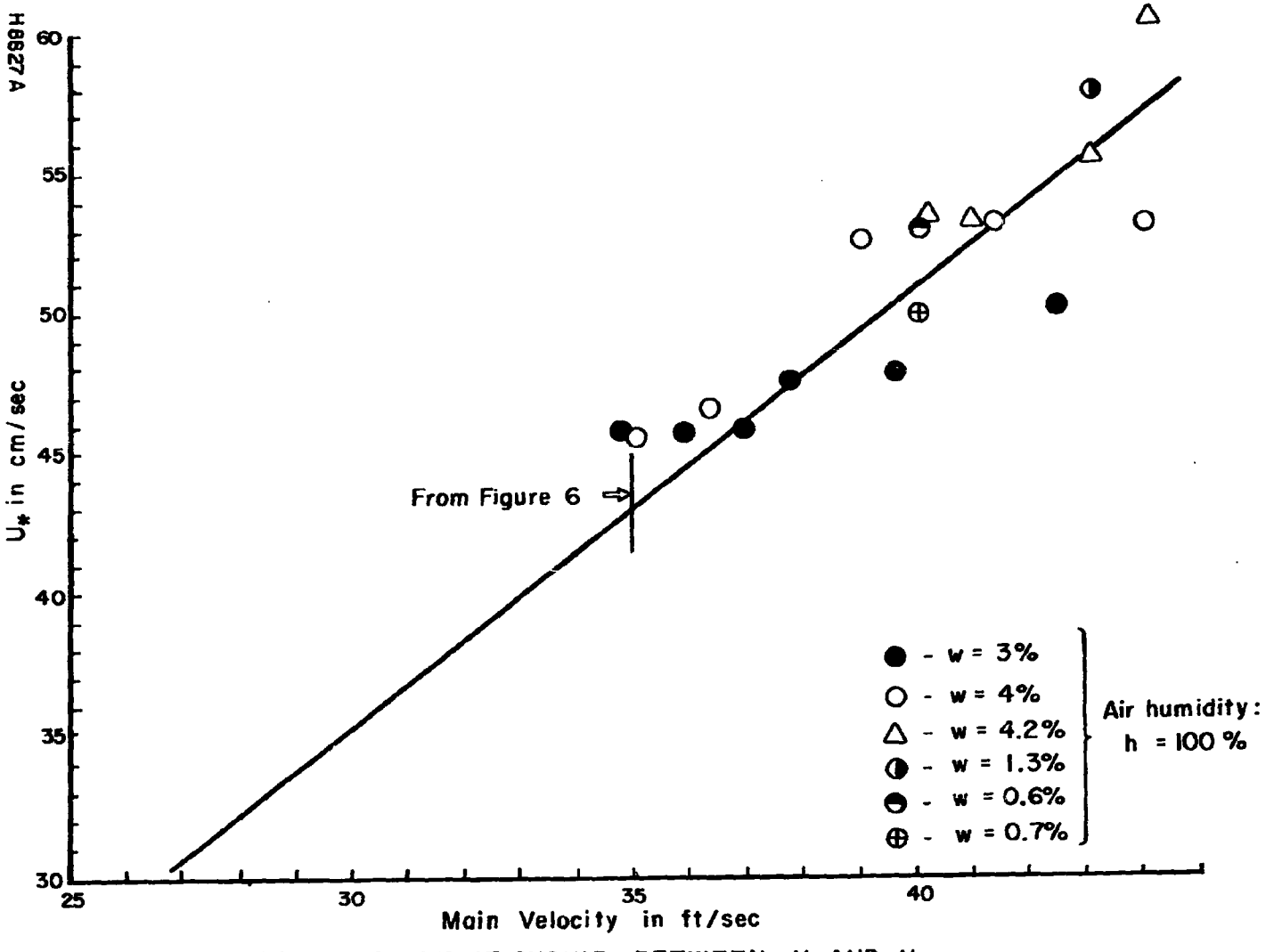

FIGURE 10

FIGURE 10- RELATIONSHIP BETWEEN U AND U_*
(FOR HIGH WATER CONTENT)

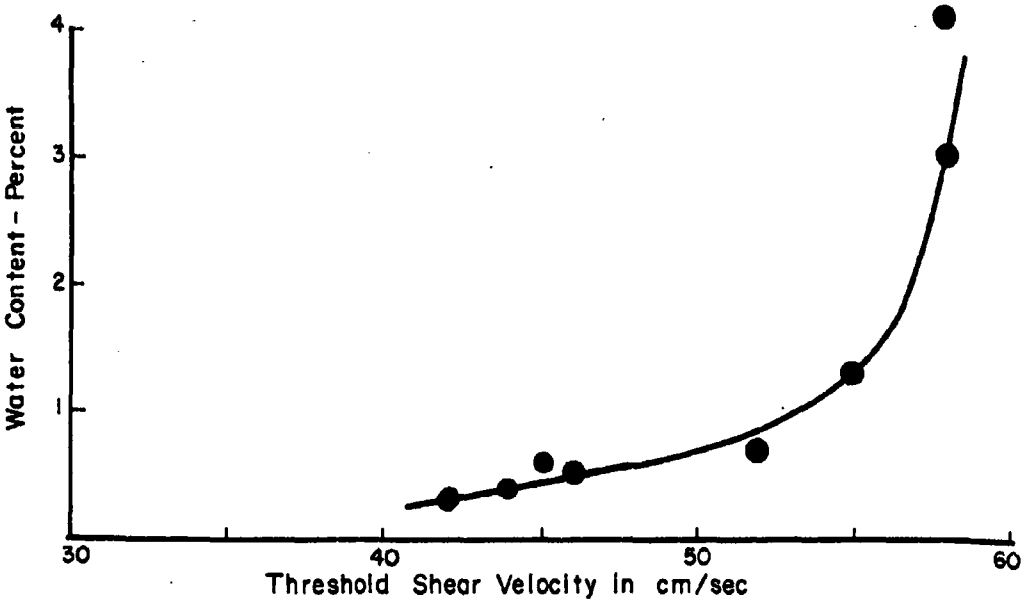

FIGURE 11 - VARIATION OF THE THRESHOLD WITH MOISTURE
(FOR HIGH WATER CONTENT)

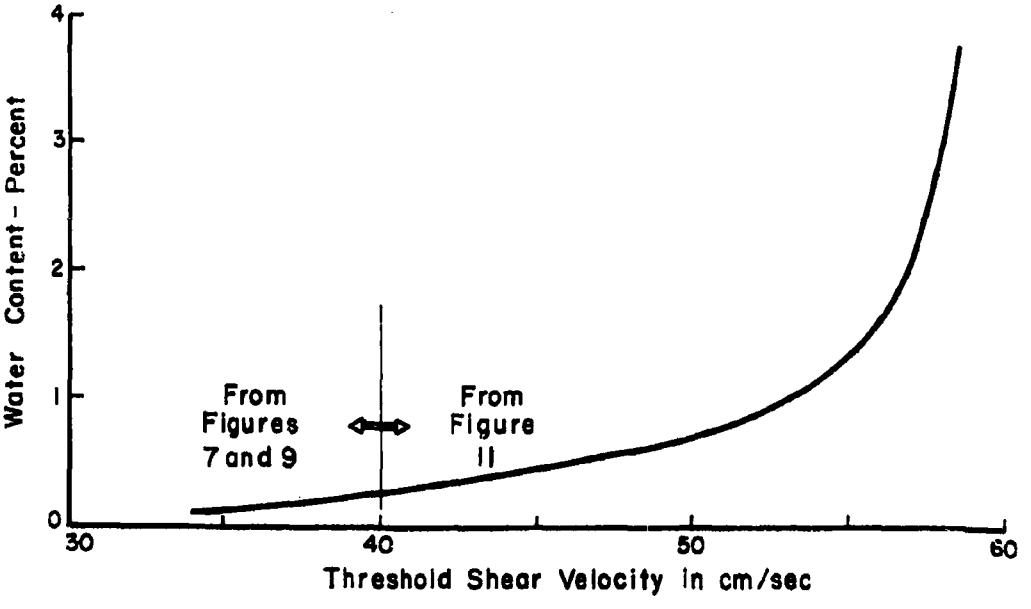

FIGURE 12 - VARIATION OF THE THRESHOLD WITH MOISTURE
(COMPLETE RESULTS)

H 8828A

FIGURES 11, 12

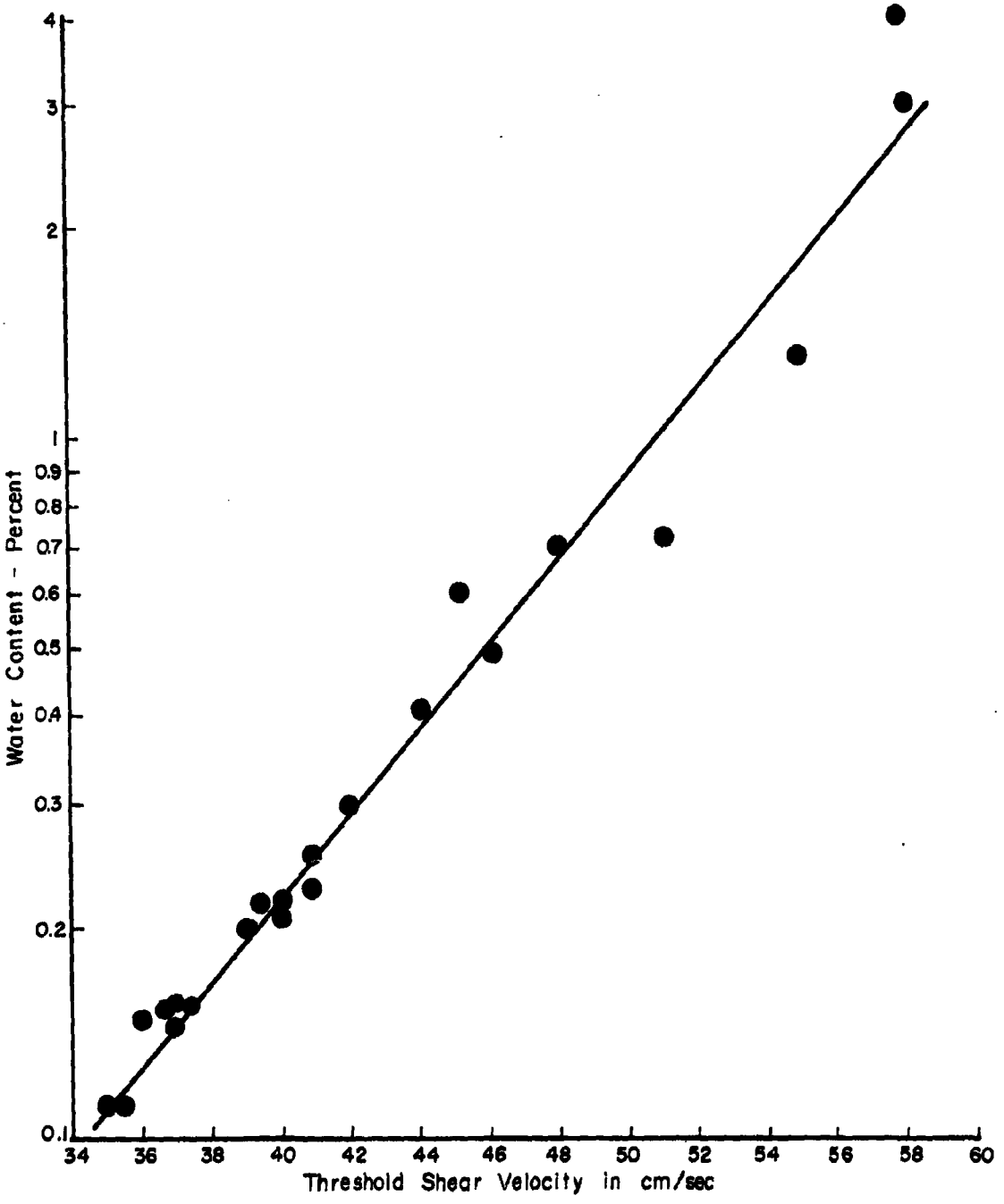

FIGURE 13 - VARIATION OF THE THRESHOLD WITH MOISTURE

H 8829A

FIGURE 13

UNCLASSIFIED

UNCLASSIFIED